Metabolic pathway analysis of an *Acinetobacter* strain capable of assimilating diverse hydrocarbons and aromatic compounds

Shori Inoue, Shogo Yoshimoto, Maiko Hattori, Shotaro Yamagishi, and Katsutoshi Hori[#]

Department of Biomolecular Engineering, Graduate School of Engineering, Nagoya University, Furo-cho, Chikusa-ku, Nagoya, Aichi 464-8603, Japan

Correspondence: Katsutoshi Hori

Department of Biomolecular Engineering, Graduate School of Engineering, Nagoya University, Furo-cho, Chikusa-ku, Nagoya, Aichi 464-8603, Japan.

Tel: +81-52-789-3339

Email: khori@chembio.nagoya-u.ac.jp

ABSTRACT

Sustainable bioproduction requires developing robust microbial chassis with broad metabolic versatility and suitability for industrial applications. *Acinetobacter* sp. Tol 5 is a highly adhesive bacterium capable of utilizing various hydrocarbons, making it a promising chassis candidate for immobilized whole-cell catalysis. In this study, we characterized the carbon metabolism of Tol 5 by reconstructing metabolic pathway maps and analyzing the transcriptomes of cells grown on ethanol, hexadecane, toluene, and phenol. Genomic analysis revealed broad metabolic pathways for alcohols, alkanes, and aromatics, including five distinct aromatic degradation routes. Transcriptome data elucidated the specific genes governing the metabolic pathways for each carbon source. Notably, during growth on phenol, both the *ortho*- and *meta*- catechol cleavage pathways were induced. While the gene disruption of the *meta*- cleavage enzyme TodE had no effect, that of toluene dioxygenase resulted in an extended lag phase but a higher final cell yield on phenol, indicating that it facilitates rapid detoxification but diverts carbon into unassimilable by-products. Furthermore, genes involved in oxidative and osmotic stress resistance were coordinately upregulated on hydrocarbon sources. These results provide a comprehensive view of the carbon metabolism of Tol 5 and reveal new aspects of microbial metabolism of hydrocarbons and aromatic compounds.

INTRODUCTION

In recent years, there has been a global shift from petrochemical synthesis to more sustainable bioprocesses, driven by the need to reduce fossil resource consumption and lessen environmental impact. Microorganisms, especially bacteria, are considered useful hosts for bioproduction due to their rapid growth, ease of genetic manipulation, and capacity for engineering to improve the productivity of valuable compounds. *Escherichia coli* is one of the most widely used microbial chassis in bioproduction, owing to its well-characterized molecular biology and metabolic systems (Pontrelli *et al.*, 2018). Concurrently, environmental microorganisms capable of assimilating non-sugar carbon substrates, such as C1 compounds, aromatic hydrocarbons, and oils, are increasingly valued for converting underutilized resources, including petrochemical by-products, agricultural waste, lignocellulosic biomass, and exhaust gases, into valuable products (Liew *et al.*, 2022, Liu *et al.*, 2024, Martín-González *et al.*, 2025). For instance, *Pseudomonas putida* is recognized for its high organic solvent tolerance and versatile catabolic pathways and has been deployed in many applications, demonstrating the immense potential of environmental isolates (Nakazawa, 2002, Nelson *et al.*, 2002, Ramos *et al.*, 2015, de Lorenzo *et al.*, 2024, Martínez-García & de Lorenzo, 2024). Therefore, it is essential to explore and develop new microbial chassis that can metabolize diverse substrates, tolerate harsh environmental conditions, and perform robustly in industrial bioprocesses.

Members of the genus *Acinetobacter* are ubiquitous and found in diverse environments, including soil, oceans, freshwater, sediments, activated sludge, and clinical settings (5, 6). The genus possesses extensive genomic plasticity, which contributes to the pathogenic potential of some species. However, this trait, combined with a high tolerance to environmental stress, has also made it a focus of great interest in environmental microbiology, where several species have shown potential in bioproduction and bioremediation. For example, *A. baylyi* ADP1 has been studied as a host for the valorization of aromatic compounds via the β-ketoadipate pathway (Biggs *et al.*, 2020, Luo *et al.*, 2022, Kurnia *et al.*, 2024). *A. venetianus* RAG-1, which has multiple alkane hydroxylase genes, exhibits a pronounced ability to degrade crude oil and has been employed in bioremediation applications (Liu *et al.*, 2021). Furthermore, *A. junii* BP25 has been utilized for the production of polyhydroxyalkanoates (PHAs) from food waste-derived organic acids, while *A. venetianus* AMO1502 has been applied in the biosynthesis of bioemulsifiers (Sabapathy *et al.*, 2019, D'Almeida *et al.*, 2024).

Acinetobacter sp. Tol 5, originally isolated as a toluene-degrading bacterium from an exhaust gas treatment reactor, can degrade various hydrocarbons, including benzene, toluene, and xylene (BTX) (Hori *et al.*, 2001). In addition to metabolic versatility, Tol 5 exhibits rapid autoagglutination and high adhesiveness to various solid materials, such as plastics, glass, and metals (Ishikawa *et al.*,

2012). This adhesive phenotype is mediated by its fibrous cell surface protein AtaA, a member of the trimeric autotransporter adhesin (TAA) family proteins (Ishikawa *et al.*, 2012). Previous studies have revealed the functional domains and biophysical properties of AtaA (Yoshimoto *et al.*, 2023, Yoshimoto *et al.*, 2024, Inoue *et al.*, 2025). Based on these findings, a reversible cell immobilization method was proposed to enhance the efficiency and productivity of bioproduction processes (Yoshimoto *et al.*, 2017). To demonstrate its utility, Tol 5 expressing heterologous biosynthetic genes was immobilized on porous carriers and successfully utilized in an unconventional gas-phase bioreaction process to produce a high-value-added monoterpenoid, (*E*)-geranic acid (Usami *et al.*, 2020). Although these advances indicate that Tol 5 is a promising microbial chassis for innovative bioproduction, its central metabolic network remains largely uncharacterized.

In this study, we characterized the carbon metabolism of Tol 5 by reconstructing metabolic pathways from the complete genome sequence and performing transcriptomic analyses of Tol 5 cells grown on ethanol, hexadecane, or aromatic compounds as the sole carbon source.

MATERIALS AND METHODS

Genome sequence data analysis

The complete genome sequence of Tol 5, consisting of a chromosome and a plasmid, was obtained from the NCBI database (accession: AP024708 and AP024709). All amino acid sequences of the coding sequences (CDSs) were searched against the UniProtKB/Swiss-Prot database (as of August 2024) using BLASTP, and the best-scoring hit for each CDS was used for functional annotation. The sequences were further searched against the KEGG database using BlastKOALA and KEGG automatic annotation server (KAAS) (accession: T11084). For CDSs that could not be annotated with the KEGG database, additional searches were performed against the EggNOG database using eggNOG-mapper. Based on the annotations obtained, a central carbon metabolic pathway map was reconstructed using KEGG mapper. Peripheral metabolic pathways, including those involved in the degradation of alkanes and aromatic compounds, were inferred by comparing operon organization with those previously characterized in closely related bacterial species. Operon structures were predicted using two tools: Operon-mapper (Taboada *et al.*, 2018), which infers operons based on intergenic distances and gene functions, and Rockhopper (McClure *et al.*, 2013), which additionally incorporates transcriptomic data. Functional annotations, operon predictions, and metabolic pathways were manually curated based on information from relevant literature.

Strains, plasmids, and culture conditions

The primers, bacterial strains, and plasmids used in this study are shown in Tables S1 and S2. *E. coli* and its transformants were cultured in lysogeny broth (LB) medium (20066-95; Nacalai Tesque, Kyoto, Japan) at 37°C. *Acinetobacter* sp. Tol 5 and its mutants were cultured in LB medium or basal salt (BS) medium (Hori *et al.*, 2001) at 28°C.

Gene knockout

The gene knockout mutants were generated using the cytidine base editing system for *Acinetobacter* according to the previous reports (Wang *et al.*, 2019, Inoue *et al.*, 2025). The DNA dimer fragment encoding the sequence of the single guide RNA was prepared by mixing oligo DNAs listed in Table S2 in 50 mM NaCl solution and gradually cooling from 95°C to 18°C at 0.1°C/s. This dimer was introduced into the BsaI site of pBECAb-apr. The constructed plasmid was electroporated into Tol 5_{REK}, a restriction-modification system and *ataA*-deficient strain (Ishikawa & Hori, 2024). After overnight culture of Tol 5_{REK} harboring the plasmid in BS medium to promote mutation, the cells were spread on a BS agar plate containing 5 % (w/v) sucrose to remove the plasmid. Mutation of the target gene was confirmed by sequencing the DNA amplified from the genome by PCR using KOD FX Neo (Toyobo, Osaka, Japan).

Bacterial cell growth

For the wild type strain of Tol 5, the cells cultured in LB medium supplemented with each carbon source were collected by centrifugation, washed with BS medium, and resuspended in BS medium. A 0.20-mL aliquot of the suspension was inoculated into 20 mL of BS medium in 100-mL Erlenmeyer flasks. Four rectangular pieces of polyurethane foam support (10 × 10 × 10 mm, CFH-20, 20 pores/25 mm; Inoac Corporation, Nagoya, Japan) were added to each flask as carriers to immobilize the cells. Each carbon source was added at a carbon equivalent concentration of 3.3×10^{-2} mol/L. The flasks were then capped with silicone stoppers for cultures containing sodium lactate, ethanol, and hexadecane, or with Viton rubber stoppers for those containing toluene and phenol. The cultures were incubated at 28°C with shaking at 115 rpm. The optical density at 660 nm (OD_{660}) was measured as previously reported (Inoue *et al.*, 2025). At each time point, flasks were collected, and the cultures were mixed vigorously with 1 mL of 10% Casamino Acids technical grade (CA-T; Becton, Dickinson and Company, Franklin Lakes, NJ, USA). The CA-T solution was added to inhibit AtaA-mediated cell aggregation and to detach the bacterial cells from the support (Ohara *et al.*, 2019). The OD_{660} of the resulting cell suspension was measured using a UV□Vis spectrophotometer (UV-1850; Shimadzu Corporation, Kyoto, Japan).

For the Tol 5_{REK} mutants, the cells cultured in LB medium supplemented with each carbon source were collected by centrifugation, washed with BS medium, and resuspended in BS medium. A 0.25-mL aliquot of the suspension was inoculated into 5 mL of BS medium in a glass test tube. Each carbon source was added at a carbon equivalent concentration of 1.4×10^{-2} mol/L, and the optical density (OD) was monitored every 60 min using the OD-monitorC&T system (Taitec, Saitama, Japan) during the culture.

RNA sequencing

Tol 5 cells were harvested from the polyurethane foam support during the late log phase (OD_{660} = 0.2–0.5). The detached cells were collected by centrifugation (8,000 × g, 4°C, 3 min), and the cell pellets were stored at -80°C. For each growth condition, three biological replicates were prepared. Total RNA was extracted using the RNA Prep Kit (Cica Genus, Tokyo, Japan) according to the manufacturer's protocol. Ribosomal RNA was removed using the NEBNext rRNA Depletion Kit (Bacteria) (New England Biolabs, Ipswich, MA, USA), and cDNA libraries were generated with the NEBNext Ultra II RNA Library Prep Kit for Illumina (New England Biolabs, Ipswich, MA, USA). The cDNA libraries were sequenced on the Illumina NextSeq550. Raw FASTQ reads were quality-filtered using fastp (version 0.23.2) and mapped to the Tol 5 genome (accession: AP024708 and AP024709) using Bowtie2 (version 2.5.1) with default parameters. Mapped reads were counted using featureCounts (version 2.0.6).

Differential gene-expression analysis

Raw read counts of CDSs were analyzed in R using the edgeR package (version 3.42.4). Genes with extremely low expression were removed using the filterByExpr function. Normalization was performed using the trimmed mean of M-values (TMM) method implemented in the calcNormFactors function. Differential gene expression analysis was conducted using the quasi-likelihood pipeline. A design matrix was constructed incorporating the cells grown on six different carbon sources (n = 3), with the data from those grown on lactate set as the reference group. Dispersion estimates were obtained using the estimateDisp function, and model fitting was performed with the glmQLFit function. Differential expression between each condition and the control condition (lactate condition) was assessed using the glmQLFTest function. Genes with false discovery rate (FDR) < 0.01, $|\log_2$ fold change (FC)$|$ > 1, and $\log_2$ counts per million (CPM) > 3 were extracted as significantly differentially expressed genes.

RESULTS

Central carbon metabolism

The complete genome of Tol 5 consists of two circular DNA components, a chromosome of 4,681,789 bp and a plasmid of 117,717 bp, collectively encoding 4,404 predicted CDSs (Ishikawa & Hori, 2021). We first evaluated the functional annotation of each CDS using multiple databases, including NCBI, UniProtKB/Swiss-Prot, KEGG, and EggNOG, as well as information from relevant literature (Table S3). Tol 5 encodes all the enzymes for gluconeogenesis, pentose phosphate pathway, tricarboxylic acid (TCA) cycle, glyoxylate shunt, purine and pyrimidine biosynthesis, β-oxidation, and fatty acid biosynthesis (Fig. 1, Table S4). In contrast, glycolysis via the Embden–Meyerhof–Parnas (EMP) pathway is incomplete due to the absence of hexokinase, phosphofructokinase, and pyruvate kinase, which is a trait commonly observed among *Acinetobacter* species (Zhao *et al.*, 2023). While some *Acinetobacter* strains, such as *A. baylyi* ADP1 and *A. baumannii*, metabolize glucose via nonspecific pyrroloquinoline quinone-dependent aldose dehydrogenase and the Entner–Doudoroff (ED) pathway (Barbe *et al.*, 2004, Kannisto *et al.*, 2015, Ren & Palmer Lauren, 2023), Tol 5 completely lacks these genes. Furthermore, *A. baumannii* ATCC 19606 metabolizes pentoses such as L-arabinose, D-xylose, and D-ribose via a pathway encoded by *ara* genes that converts them into α-ketoglutarate (Alberti *et al.*, 2023), but Tol 5 also lacks the *ara* genes. These results suggest that Tol 5 has a very limited capacity for sugar utilization as carbon sources.

Many *Acinetobacter* strains utilize organic acids and fatty acids as carbon sources (Ren & Palmer Lauren, 2023). Tol 5 possesses three acetate assimilation routes, including the reversible acetate kinase-phosphotransacetylase (AckA-Pta) pathway, the irreversible acetyl-CoA synthetase (ACS) pathway, and the reversible pathway mediated by succinyl-CoA:coenzyme A transferase AarC (Fig. 1, Table S4). For fatty acid degradation, multiple candidate genes corresponding to each step of β-oxidation were identified, including two putative acyl-CoA ligases, twelve acyl-CoA dehydrogenases, four enoyl-CoA hydratases, and three thiolases. Propionyl-CoA generated during the β-oxidation of odd-chain fatty acids was predicted to be catabolized to succinate and pyruvate via the methylcitrate cycle, which consists of 2-methylisocitrate lyase (PrpB), 2-methylcitrate synthase (PrpC), 2-methylcitrate dehydratase (AcnD), 2-methylaconitate isomerase (PrpF), and bifunctional aconitate hydratase/isomerase (AcnA and/or AcnB). In addition, four extracellular lipase genes were identified in Tol 5 (Table S1), all of which are tandemly arranged (*TOL5_03740–TOL5_03770*) and share 44–52% amino acid sequence identities with the triacylglycerol lipase Lip reported in *P. aeruginosa* PAO1 (Wohlfarth *et al.*, 1992). Tol 5 further encodes key enzymes that redirect fatty acid oxidation intermediates into carbon storage compounds. A bifunctional wax ester synthase/acyl-CoA:diacylglycerol acyltransferase (WS/DGAT, AtfA)

mediates the production of wax esters and triacylglycerols, while polyhydroxyalkanoate (PHA) synthase (PhaC) is responsible for the production of PHAs.

Alkane metabolism

Under aerobic conditions, *n*-alkanes are first oxidized at their terminal methyl group to primary alcohols by alkane hydroxylases, and these alcohols are then further oxidized to aldehydes and finally to fatty acids (Rojo, 2009). The Tol 5 chromosome encodes multiple alkane hydroxylases, including a membrane-bound non-heme iron alkane monooxygenase AlkB, and three flavin-containing monooxygenases encoded by *almA*, *ladA_1*, *ladA_2* (Table S4). Additionally, the plasmid of Tol 5 carries a gene encoding an alkane hydroxylase (*TOL5_43480*), whose amino acid sequence shares 99% identity with that of a cytochrome P450 monooxygenase of the CYP153 family found in *Acinetobacter* sp. EB104 (Maier *et al.*, 2001). It also includes genes encoding associated redox partners, ferredoxin (*TOL5_43490*) and ferredoxin reductase (*TOL5_43470*). AlkB and CYP153 typically oxidize short- and medium-chain *n*-alkanes (C16 or less), whereas AlmA and LadA act on long-chain *n*-alkanes (C20 or more) (Nie *et al.*, 2014, Kong *et al.*, 2021, Chen *et al.*, 2024). The resulting primary alcohols are further oxidized by alcohol dehydrogenases (ADHs) and aldehyde dehydrogenases (ALDHs). In Tol 5 genome, at least six putative ADH genes and one ALDH gene were predicted to be involved in fatty alcohol and fatty aldehyde oxidation (Table S4). Although the functions of most ADHs in Tol 5 remain unclear, the iron-containing ADH encoded by *yiaY_1* shares 91% amino acid sequence identity with ADH4 from *A. baumannii* ATCC 19606, which catalyzes the oxidation of ethanol, 1-propanol, and 1-butanol (Lin *et al.*, 2021). The putative ALDH encoded by *aldB* (AldB) shares 87% amino acid identity with a long-chain ALDH, Ald1, reported in *Acinetobacter* sp. M-1 (46).

Aromatic compounds metabolism

Genes encoding multi-component oxygenases for aromatic compound oxidation, as well as enzymes for successive reaction steps leading to central metabolites, are generally organized into operons and regulated by specific transcriptional regulators (Phale *et al.*, 2020). Based on the predicted operons involved in aromatic compound degradation (Table S4, Fig. 2), we reconstructed the aromatic degradation pathways in Tol 5, identifying five major aromatic degradation routes (Fig. 3).

The *pca* genes encode the enzymes responsible for the degradation of protocatechuate (PCA pathway) (Fig. 3), forming a gene cluster together with the aromatic compounds transport protein PcaK and the transcriptional repressor PcaU (Fig. 2). The *cat* gene cluster encodes the enzymes

responsible for the degradation of catechol (CAT pathway) (Fig. 3) and the transcriptional activator CatM (Fig. 2). Protocatechuate and catechol are common intermediates derived from various aromatic compounds through various upstream pathways. The PCA and CAT pathways funnel these intermediates into acetyl-CoA and succinyl-CoA via oxidative *ortho*-cleavage of aromatic ring, serving as central routes for aromatic compound degradation that are widely conserved in *Acinetobacter* species (Barbe *et al.*, 2004, Fischer *et al.*, 2008, Stuani *et al.*, 2014, Breisch *et al.*, 2022). In Tol 5, the *pca* genes are located adjacent to the *qui* genes (Fig. 2), which encode enzymes that convert quinate and shikimate to protocatechuate (Fig. 3). The structure of this gene cluster is similar to that reported in *A. baylyi* ADP1 (Dal *et al.*, 2005), and as described for ADP1, the *pca* and *qui* genes are likely organized as a large single operon under the regulator PcaU in Tol 5. Tol 5 also possesses the *pob* and *van* genes, which encode upstream pathways leading to protocatechuate, along with their respective transcriptional regulators (PobR and VanR) (Fig. 2 and 3). The *cat* genes are located adjacent to the *mph* gene cluster, which encodes the components of the phenol monooxygenase complex MphKLMNOP, catechol 1,2-dioxygenase CatA (encoded by *catA_2*), and the regulatory proteins MphX (repressor) and MphR (activator) (Fig. 2). The structure of the *mph* operon in Tol 5 resembles that of *A. calcoaceticus* PHEA-2 (Yu *et al.*, 2011), but is distinguished by the presence of the additional *catA* gene (*catA_2*) located immediately downstream in the same operon. In addition, Tol 5 possesses the *ben* and *iac* genes, which encode enzymes for the upstream pathways that lead to catechol, along with their respective transcriptional regulators (BenM and IacR) and transporters (BenE, BenK, and a putative transporter encoded by *TOL5_19290*) (Fig. 2 and 3). Notably, the *ben* genes in Tol 5 are located over 900 kbp away from the *cat* operon, in contrast to *A. baylyi* ADP1, in which the *ben* genes are located adjacent to the *cat* genes to facilitate coordinated regulation of gene expression (Bleichrodt *et al.*, 2010). Despite its distinct genomic location, the *ben* operon in Tol 5 includes the third *catA* gene (encoded by *catA_4*), indicating that coordinated regulation between the *ben* and *cat* genes is maintained.

The *tod* operon encodes the enzymes responsible for the degradation of alkylbenzene (TOD pathway) (Fig. 3) and is located between the *todS*-*todT* two-component regulatory system and the putative toluene transporter gene *fadL2*, which is located in a separate operon (Fig. 2). In the TOD pathway, alkylbenzene is oxidized into 3-alkylcatechol. The aromatic ring is then opened via oxidative *meta*-cleavage, and in the case of toluene, the intermediates are ultimately converted into acetate, pyruvate, and acetyl-CoA. Although rarely found in other *Acinetobacter* species, the *tod* genes of Tol 5 share high similarity with those of *P. putida* strains and play a central role in the degradation of toluene and benzene (Yoshimoto *et al.*, 2025).

Furthermore, Tol 5 possesses the *paa* genes, which encode the enzymes responsible for the degradation of phenylacetic acid (PAA pathway) (Fig. 3), as well as the transcriptional repressor

PaaX (Fig. 2). The PAA pathway degrades phenylacetate via epoxidation of CoA thioesters. While this pathway in *A. baumannii* strains is thought to be primarily associated with phenylalanine degradation (Teufel *et al.*, 2010, Hooppaw Anna *et al.*, 2022), Tol 5 lacks the enzymes required to convert phenylalanine to phenylacetate.

In addition, Tol 5 also possesses a gene cluster encoding a putative homogentisate degradation route (HMG pathway) (Fig. 3), which includes 4-hydroxyphenylpyruvate dioxygenase (HPD), an IclR-type transcriptional repressor (IclR), maleylacetoacetate isomerase (MaiA), fumarylacetoacetase (FahA), 3-oxoacid CoA-transferase subunits A and B (ScoA and ScoB), and an aromatic amino acid transporter (AroP), as well as a putative homogentisate dioxygenase encoded by *TOL5_11140* (Fig. 2). Although the protein product of *TOL5_11140* was annotated as a glyoxalase (Table S1), it shares 22.7% amino acid identity with homogentisate 1,2-dioxygenase HmgA (B7VA96) and 18.8% amino acid identity with metapyrocatechase XylE (Q04385) from *P. putida*. Based on the genomic context, the HMG pathway in Tol 5 is likely involved in tyrosine metabolism.

Substrate-dependent transcriptomic responses to lactate, ethanol, and hexadecane

While genomic analysis revealed that Tol 5 possesses multiple genes involved in the metabolism of alcohols and alkanes, the expression of key enzymes, such as alcohol dehydrogenases and alkane hydroxylases, is generally subject to strict regulation depending on the available carbon source. To identify the specific genes induced for their assimilation, we performed transcriptome analysis. Ethanol and hexadecane were selected as a representative short-chain alcohol and long-chain alkane, respectively, and Tol 5 cells were cultured in BS medium supplemented with each carbon source (Fig. S1A and B). Because Tol 5 cells exhibit autoagglutination and high adhesiveness in BS medium, polyurethane support was used to immobilize the cells as previously reported (Hori *et al.*, 2011). Cells were harvested from the support during the late log phase, and their transcriptomes were compared with those of cells grown on lactate (Table S5 and S6). Differentially expressed genes were defined by the thresholds of $|\log_2 FC| > 1$, $\log_2 CPM > 3$, and $FDR < 0.01$ (Fig. 4A, Table S7).

In ethanol culture, 14 genes were significantly upregulated, including *yiaY_1* and *aldB*, which encode an iron-containing ADH and a putative ALDH, respectively (Table S7). Since *yiaY_1* was the only ADH gene induced by ethanol, it is likely the primary ADH responsible for ethanol oxidation in Tol 5 (Fig. 4B). Although AldB shares 87% amino acid identity with Ald1 from *Acinetobacter* sp. M-1, which has been characterized as a long-chain ALDH that is inactive toward short-chain substrates such as acetaldehyde (Ishige *et al.*, 2000), its induction during growth on ethanol suggests that AldB functions differently from Ald1 and catalyzes acetaldehyde oxidation in Tol 5. Regarding the conversion of acetate into acetyl-CoA, although Tol 5 possesses both the AckA-Pta pathway and

the ACS pathway (Fig. 1), genes in neither pathway were significantly upregulated (Fig. 4B). Thus, the primary acetate conversion pathway into acetyl-CoA in Tol 5 during growth on ethanol could not be determined in this study. Additionally, *aceA*, which encodes isocitrate lyase of the glyoxylate shunt that bypasses the decarboxylation steps of the TCA cycle and conserves carbon flux for gluconeogenesis (Fig. 1), was upregulated. A similar regulatory pattern was observed in *Acinetobacter oleivorans* DR1, where the *aceA* was upregulated during growth on acetate (Park *et al.*, 2019), suggesting that Tol 5 employs a similar strategy for assimilating acetate generated from ethanol.

In hexadecane culture, 266 genes were significantly upregulated (Table S7). Among the multiple alkane hydroxylase genes in Tol 5, *alkB* and the CYP153 gene were specifically induced, indicating their involvement in the initial hydroxylation of hexadecane (Fig. 4C). The gene *yiaY_3*, encoding an iron-containing ADH, and *calB*, encoding a putative coniferyl aldehyde dehydrogenase, were also upregulated, suggesting their roles in the oxidation of hexadecanol to hexadecanal and subsequently to hexadecanoic acid. The genes involved in every step of the β-oxidation pathway were upregulated. Among the multiple predicted enzymes for each step, only *fagA*, *fadB*, *fadD4* (one of the two predicted acyl-CoA ligase genes), *fadE*, and *ydiO_5* (two of the twelve predicted acyl-CoA dehydrogenase genes) were specifically induced (Fig. 4C).

Twenty-one genes were downregulated in both ethanol and hexadecane cultures compared to lactate culture, implying that these genes are specifically upregulated during growth on lactate (Table S7 and S8). Among them, the *lldP*, *lldR*, *lldD_1*, and *dld* genes (Fig. 1 and Table S8), which form an operon similar to the *lldPRD* operon involved in lactate metabolism reported in *A. baumannii*, were identified (Morris *et al.*, 2024). The *aceE* and *aceF* genes, which encode components of pyruvate dehydrogenase, were also upregulated during growth on lactate. The *pca* and *qui* genes, responsible for quinate and shikimate utilization, were downregulated in ethanol and hexadecane cultures, indicating catabolite repression similar to that reported for *A. baylyi* ADP1, where these genes are repressed in the presence of preferred carbon sources (Fischer *et al.*, 2008, Bleichrodt *et al.*, 2010).

Substrate-specific regulation of aromatics degradation pathways

Subsequently, we focused on the transcriptional regulation of the aromatic degradation pathways in Tol 5, particularly for the degradation of toluene and phenol, which are valuable substrates for the bioproduction of aromatic-derived fine chemicals. Tol 5 cells were cultured in BS medium supplemented with toluene or phenol (Fig. S1C) and subjected to transcriptome analysis using the same procedure described above. The resulting data were also compared with those of cells grown on lactate (Fig. 5A, Table S6).

In toluene and phenol cultures, 349 and 643 genes were upregulated, while 292 and 578 genes were downregulated, respectively (Table S7). Regarding the aromatic degradation pathways, toluene culture strongly induced only the *tod* operon, including all of the TOD pathway genes (Fig. 5B). Expression levels of genes in the other aromatic degradation pathways did not differ significantly (Fig. 5B and S2). Although genes in the *mph* operon (encoding phenol monooxygenase) and the *paa* operon (encoding the PAA pathway) showed slight upregulation, their induction levels were negligible compared to those of the *tod* operon. The *fadL2*, which is located adjacent to the *tod* operon and encodes a putative toluene transporter (Fig. 2), was also upregulated (Fig. 5B). Although it was reported that its deletion did not affect growth on toluene (Yoshimoto *et al.*, 2025), this strong induction suggests its involvement in toluene assimilation. A previous study has shown that disruption of *todC1* completely abolishes growth on toluene (Yoshimoto *et al.*, 2025). Consistent with this phenotypic evidence and our genomic predictions, these transcriptional responses indicate that toluene degradation proceeds exclusively through the TOD pathway (Fig. 5C). In contrast, in phenol culture, both the *mph-cat* gene cluster, which comprises the predicted phenol degradation pathway, and the *tod* operon were significantly upregulated (Fig. 5B). Notably, the induction levels of the tod genes reached those observed in toluene culture. Most genes of the PCA, PAA, and HMG pathways were not significantly changed in phenol culture (Fig. S2). Although phenol is predicted to be metabolized via hydroxylation by phenol monooxygenase and the CAT pathway, encoded by the *mph-cat* gene cluster (Fig. 3), this transcriptional cross-regulation suggests that phenol might also be degraded via *tod* enzymes, including toluene dioxygenase and the catechol *meta*-cleavage pathway (Fig. 5D).

Aromatic substrates also influenced downstream central metabolic pathways (Fig. S3, Table S7). Growth on these compounds triggered a differential response in aconitate hydratase isozymes; *acnA_2* was upregulated, whereas the expression of *acnB* was not significantly changed. Given that this pattern was also observed during growth on hexadecane, the upregulation of *acnA_2* appears to be a common response to hydrocarbon utilization. Concurrently, *pckG*, encoding the key gluconeogenic enzyme phosphoenolpyruvate carboxykinase (Sauer & Eikmanns, 2005) (Fig. 1), was downregulated in both toluene and phenol cultures, indicating reduced carbon flux from the TCA cycle into gluconeogenesis compared to cells grown on lactate. In phenol culture, *mqo*, encoding malate:quinone oxidoreductase, was specifically upregulated, while *mdh*, encoding NAD-dependent malate dehydrogenase, was downregulated (Fig. S3). Both enzymes catalyze the conversion of malate to oxaloacetate; however, Mqo transfers electrons directly to the quinone pool, while Mdh reduces NAD^+ to generate NADH. This transcriptional switching suggests that during phenol assimilation, Tol 5 modulates malate conversion routes to manage the cellular redox balance.

Expression of intracellular stress resistance genes under different carbon sources

In addition to carbon metabolic pathways, genes involved in environmental stress resistance showed significant transcriptional changes depending on the carbon source (Fig. 6, Table S7). Notably, several genes related to oxidative stress resistance were upregulated in Tol 5 cells grown on hexadecane, toluene, and phenol. Genes encoding monofunctional heme catalases (*katA* and/or *katE*) were highly upregulated under all three conditions. In hexadecane culture, the Mn/Fe superoxide dismutase genes (*sodA_1* and/or *sodA_2*) were repressed. In contrast, during growth on phenol, the *sodA_2* was significantly upregulated along with the periplasmic Cu/Zn superoxide dismutase gene (*sodC*). These superoxide dismutase genes were also weakly upregulated in toluene culture. The alkyl hydroperoxide reductase gene (*ahpC_1*), which plays a role in peroxide detoxification, was highly upregulated in phenol culture. Concurrently, the trehalose synthesis genes (*otsA* and *otsB*), associated with osmotic stress resistance (Zeidler *et al.*, 2017, Liu *et al.*, 2025), were also upregulated during growth on all three alkane and aromatic carbon sources. The *otsB* gene, which encodes trehalose-6-phosphate phosphatase, exhibited low expression levels (log□ CPM) but showed high upregulation ($\log_2$ FC). The upregulation of oxidative stress resistance and trehalose synthesis genes has been reported in *A. oleivorans* DR1 during triacontane metabolism (Park *et al.*, 2019). Our findings demonstrate that the upregulation of stress resistance genes represents a more general adaptation strategy induced not only by alkanes but also by aromatic compounds such as toluene and phenol, suggesting that these stress responses constitute a fundamental mechanism required for cells to metabolize such substrates.

Growth abilities of *tod* and *mph* gene disruption mutants on toluene and phenol

Transcriptome analysis of Tol 5 cells grown on aromatic substrates revealed that while toluene culture induces only the *tod* genes with high specificity, phenol culture induces both the *tod* operon and the *mph-cat* gene cluster. This transcriptional cross-regulation suggested multiple potential phenol assimilation routes; specifically, phenol might also be degraded via *tod* enzymes, including toluene dioxygenase and the *meta*-cleavage pathway (Fig. 5D). Thus, to evaluate the contribution of these pathways to growth on phenol, we used gene disruption mutants of the Tol 5_{REK} strain targeting the *tod* genes (Δ*todC1* and Δ*todE*) and the *mph* gene (Δ*mphN*). Tol 5_{REK} carries mutations in the restriction-modification system and the *ataA* gene, enabling easier genetic manipulation and reducing cell adhesion, which is necessary for the accuracy of growth evaluation. The *todC1* and *todE* encode the large subunit of the toluene dioxygenase complex and a catechol 2,3-dioxygenase, respectively, while *mphN* encodes the large subunit of the phenol monooxygenase complex.

In phenol culture, the Δ*todC1* mutant exhibited retarded growth but a higher cell yield (Fig. 7). This

indicates that while toluene dioxygenase facilitates phenol utilization, likely through phenol hydroxylation, its activity simultaneously reduces the efficiency of assimilating the carbon substrate into cellular components. However, the disruption of *mphN* (Δ*mphN*) completely abolished growth. This indicates that the phenol monooxygenase is the primary phenol hydroxylation route and that toluene dioxygenase cannot fully compensate for its absence. Furthermore, the Δ*todE* mutant showed no significant change in growth rate in phenol culture. This suggests that while the upstream toluene dioxygenase complex functions to hydroxylate phenol, the subsequent *meta*-cleavage reaction is not essential for phenol assimilation in Tol 5.

On the other hand, consistent with the specific induction of the *tod* operon observed in our transcriptome analysis, the disruption of *todC1* abolished growth in toluene culture, while the *mphN* disruption had no effect on growth in toluene culture (Fig. 7). None of these mutations affected growth in lactate culture. These results demonstrated that the observed growth defects are not due to a general loss of cellular viability.

DISCUSSION

Members of the genus *Acinetobacter* inhabit diverse environments, including soil, oceans, freshwater, sediments, activated sludge, and polluted sites (Mateo-Estrada *et al.*, 2019, Zhao *et al.*, 2023). Several *Acinetobacter* strains, such as the *A. calcoaceticus–A. baumannii* complex, are also opportunistic nosocomial pathogens that exhibit multidrug resistance (Vijayakumar *et al.*, 2019). Consequently, most previous research on *Acinetobacter* species has focused on antibiotic resistance, genomic plasticity, horizontal gene transfer, and pathogenicity, whereas the metabolic capabilities of this genus remain comparatively underexplored (Mateo-Estrada *et al.*, 2019, Zhao *et al.*, 2023). Although *A. baylyi* ADP1 is a widely used model strain and its 3.5 Mb genome has been well characterized (Barbe *et al.*, 2004, Durot *et al.*, 2008), this genome is smaller than those of many other *Acinetobacter* species, and thus represents only a subset of the metabolic potential present across the genus (Barbe *et al.*, 2004, Zhao *et al.*, 2023). In this study, we characterized the carbon metabolism of the highly adhesive hydrocarbon-degrading *Acinetobacter* strain Tol 5, which has a 4.8 Mb genome (Ishikawa & Hori, 2021). Genome analyses revealed that Tol 5 has limited capability to metabolize sugars but possesses an extensive repertoire of genes for alkane and aromatic metabolism. Tol 5 has multiple types of hydrocarbon oxygenases, including alkane monooxygenase, aromatic oxygenase, and cytochrome P450, which allow this strain to assimilate a wide range of hydrocarbons and their oxidized derivatives. Notably, we also identified the five distinct aromatic degradation routes, combining pathways broadly conserved in the genus *Acinetobacter* with additional pathways (such as TOD and HMG) that are rare in this genus. This

indicates metabolic versatility comparable to that of *P. putida* strains, widely used chassis for aromatic compound bioconversion (Nelson *et al.*, 2002, Nogales *et al.*, 2017, Martínez-García & de Lorenzo, 2024), highlighting its utility as a microbial chassis for bioproduction using aromatic compounds.

Acinetobacter species widely exhibit the capacity for alkane degradation, as more than 95% of strains encode the alkane monooxygenases AlkB and AlmA (Zhao *et al.*, 2023). Oil-degrading strains such as *A. venetianus* RAG-1 and *A. oleivorans* DR1 possess multiple AlkB homologs, enabling efficient utilization of *n*-alkanes (Park *et al.*, 2017, Liu *et al.*, 2021). Although Tol 5 possesses only one *alkB* gene on the genome, it also carries a plasmid-encoded cytochrome P450 monooxygenase of the CYP153 family. CYP153, which is a distinct alkane hydroxylase targeting short- and medium-chain *n*-alkanes, is typically found in alkane-degrading bacteria lacking AlkB but is relatively rare among *Acinetobacter* genomes (van Beilen Jan *et al.*, 2006, Nie *et al.*, 2014). Both *alkB* and the CYP153 gene were induced in Tol 5 grown on hexadecane, indicating that Tol 5 employs both types of alkane hydroxylases to oxidize hexadecane efficiently (Fig. 4C and Table S7).

Regarding aromatic metabolism in *Acinetobacter* species, two main *ortho*-cleavage pathways of catechols, encoded by *pca* and *cat* genes, have been mainly studied (Barbe *et al.*, 2004, Fischer *et al.*, 2008, Stuani *et al.*, 2014, Breisch *et al.*, 2022). Typically, the *cat* operon is located adjacent to the *ben* operon, and their expression is coordinately regulated to prevent the accumulation of catechol, which is toxic at high concentration (Jiménez *et al.*, 2014). Specifically, the catechol 1,2-dioxygenase, encoded by *catA* within the ben operon, converts the catechol generated by benzoate oxidation into *cis,cis*-muconate, which subsequently activates the downstream cat operon (Cosper Nathaniel *et al.*, 2000, Bundy *et al.*, 2002, Silva-Rocha & de Lorenzo, 2012). In Tol 5, however, the *cat* operon is located adjacent to the *mph* operon instead of the *ben* operon (Fig. 2). Furthermore, this adjacent *mph* operon contains an additional *catA* gene (*catA_2*), representing a genetic organization distinct from the *mph* operon previously reported in *A. calcoaceticus* PHEA-2 (Yu *et al.*, 2011). Analogous to the coordinated regulation seen in typical *ben-cat* clusters, the presence of this *catA* gene within the *mph* operon is likely essential for proper coordination with the downstream *cat* operon, ensuring the smooth conversion of the catechol derived from phenol without toxic accumulation. In addition, Tol 5 possesses a separate *ben* operon that also contains a *catA* gene (*catA_4*) located at a different chromosomal locus (Fig. 2). Therefore, the unique organization of the *mph* operon as well as the *ben* operon in Tol 5 likely enables fine-tuned transcription of the genes involved in the degradation of phenol and probably benzoate, representing an optimized gene organization for the degradation of aromatic compounds.

Aromatic compounds with alkyl substitutes are typically degraded via the *meta*-cleavage pathway, which has mainly been studied in *P. putida* (Zylstra *et al.*, 1988, Assinder & Williams, 1990). Tol 5

likely acquired these *tod* genes through horizontal gene transfer, making this strain unique within the genus *Acinetobacter* (Yoshimoto *et al.*, 2025). In the TOD pathway, the genes encoding all reaction steps for toluene degradation, from the initial oxidation catalyzed by toluene dioxygenase to the generation of pyruvate and acetyl-CoA, are clustered in a single *tod* operon (Fig. 2). Transcriptome analysis of Tol 5 revealed that growth on toluene strongly induced the *tod* operon, whereas the *mph* operon was slightly induced (Fig. 5B). This regulatory response is likely essential for survival because if alkyl-substituted catechols derived from toluene were processed via the *ortho*-cleavage pathway, they would be converted into dead-end metabolites such as methylmuconolactone (Taeger *et al.*, 1988). Thus, the specific induction of the *tod* operon prevents the metabolic flux from entering the unproductive *ortho*-pathway.

In contrast to the response to toluene, Tol 5 exhibited a distinct transcriptional pattern during growth on phenol. Phenol induced not only the *cat* and *mph* genes but also the *tod* genes (Fig. 5B). Interestingly, the disruption of *todC1*, encoding the large subunit of toluene dioxygenase, resulted in retarded growth and a higher final cell yield on phenol (Fig. 7). Previous studies have demonstrated that the toluene dioxygenase complex TodABC1C2 oxidizes phenol to both catechol and hydroquinone (Höring *et al.*, 2016). Based on this, we hypothesize that, in Tol 5, the upregulation of toluene dioxygenase facilitates rapid cell growth by promoting the hydroxylation of toxic phenol. However, this rapid hydroxylation comes at the cost of substrate conversion efficiency, as a portion of the phenol is converted into a likely unavailable by-product, such as hydroquinone, diverting the carbon source away from the productive *ortho*-cleavage pathway. Furthermore, a mutant lacking phenol monooxygenase (Δ*mphN*) completely failed to grow on phenol (Fig. 7). This indicates that the conversion of phenol by toluene dioxygenase alone is insufficient for its utilization as a carbon source, possibly because a high proportion of phenol is converted into hydroquinone, for which no assimilation routes were identified in Tol 5. Taken together, these results indicate that the phenol monooxygenase is the primary route for phenol metabolism in Tol 5, while toluene dioxygenase functions primarily as an auxiliary enzyme that supports rapid degradation. This stands in contrast to *P. putida* F1, where the toluene dioxygenase has been recognized as the primary enzyme for phenol degradation (Spain *et al.*, 1989, Höring *et al.*, 2016). Therefore, we propose a fundamentally different physiological role for the *tod* genes in Tol 5, with the toluene dioxygenase functioning primarily as a rapid detoxification mechanism rather than an assimilatory pathway.

Alkane and aromatic oxygenases catalyze the initial oxidation of their substrates by forming transient radicals at the active site, which can lead to the leakage of reactive oxygen species (ROS) (Sazykin *et al.*, 2016). Consequently, ROS are considered to be by-products of alkane and aromatic hydroxylation, and cells must deploy protective mechanisms to scavenge them. For instance, *A. calcoaceticus* grown on hydrocarbons exhibits increased superoxide dismutase activity, while both *A.*

oleivorans DR1 cultured on triacontane and *Paraburkholderia xenovorans* p2-fldX1 grown on 4-hydroxyphenylacetate upregulate multiple ROS scavengers (Sazykin *et al.*, 2016, Park *et al.*, 2017, Rodríguez-Castro *et al.*, 2024). In Tol 5 grown on hexadecane or aromatic compounds, oxidative stress resistance genes, including *sodA_2*, *sodC*, *katA*, *katE*, and *ahpC_1*, were induced (Fig. 6). Furthermore, the expression of TCA cycle enzymes is also likely to be adjusted according to the intracellular oxidative stress. In *E. coli*, ROS-sensitive aconitate hydratase AcnB functions as the primary aconitate hydratase during the growth phase, while ROS-tolerant isozyme AcnA is induced under oxidative stress conditions to maintain the TCA cycle (Cunningham *et al.*, 1997, Jordan *et al.*, 1999). Thus, the expression shift from *acnB* to *acnA_2* in the TCA cycle of Tol 5 grown on aromatic compounds suggests that Tol 5 also switches metabolic enzymes to maintain central metabolism (Fig. S3). In summary, Tol 5 responds to oxidative stress according to the available carbon source, not only by activating stress resistance genes but also by shifting reliance to ROS-tolerant isozymes to sustain central metabolism.

In conclusion, Tol 5 possesses a diverse set of metabolic pathways for alkanes and aromatic compounds, regulates these pathways according to available carbon sources, and activates stress resistance genes. Owing to its strong adhesiveness, ability to metabolize alkanes and aromatic compounds, and high tolerance to toxic intermediates, Tol 5 represents a promising microbial chassis for bioprocesses utilizing non-sugar substrates.

ACKNOWLEDGMENTS

The authors wish to acknowledge the Center for Gene Research, Nagoya University, for technical support with the RNA sequencing. The authors also thank Yuki Ohara for kindly discussing genome sequence data analysis and reviewing the manuscript.

This research was supported by the Graduate Program of Transformative Chem-Bio Research at Nagoya University supported by MEXT (WISE Program) to SI, the Japan Science and Technology Agency (JST) SPRING (Grant Number JPMJSP2125) to SI, the Japan Society for the Promotion of Science (JSPS) KAKENHI (Grant Number JP24H00043 and JP25K24646) to KH and SY, and the GteX Program Japan Grant number JPMJGX23B4 to KH.

AUTHOR CONTRIBUTIONS

Shori Inoue: Conceptualization, Formal analysis, Investigation, Data curation, Writing - Original Draft. **Shogo Yoshimoto:** Conceptualization, Writing - Review & Editing. **Maiko Hattori:**

Investigation. **Shotaro Yamagishi:** Investigation. **Katsutoshi Hori:** Conceptualization, Supervision, Project administration, Writing - Review & Editing.

DATA AVAILABILITY

RNA-seq data reported are available in the DDBJ Sequenced Read Archive under the accession numbers PRJDB35996.

REFERENCES

Alberti L, König P, Zeidler S, Poehlein A, Daniel R, Averhoff B & Müller V (2023) Identification and characterization of a novel pathway for aldopentose degradation in *Acinetobacter baumannii*. *Environmental Microbiology* **25**: 2416-2430.

Assinder SJ & Williams PA (1990) The TOL Plasmids: Determinants of the Catabolism of Toluene and the Xylenes. *Advances in Microbial Physiology,* Vol. 31 (Rose AH & Tempest DW, eds.), pp. 1-69. Academic Press.

Barbe V, Vallenet D, Fonknechten N, *et al.* (2004) Unique features revealed by the genome sequence of *Acinetobacter* sp. ADP1, a versatile and naturally transformation competent bacterium. *Nucleic Acids Research* **32**: 5766-5779.

Biggs BW, Bedore SR, Arvay E, Huang S, Subramanian H, McIntyre EA, Duscent-Maitland CV, Neidle EL & Tyo Keith E J (2020) Development of a genetic toolset for the highly engineerable and metabolically versatile *Acinetobacter baylyi* ADP1. *Nucleic Acids Research* **48**: 5169-5182.

Bleichrodt FS, Fischer R & Gerischer UC (2010) The β-ketoadipate pathway of *Acinetobacter baylyi* undergoes carbon catabolite repression, cross-regulation and vertical regulation, and is affected by Crc. *Microbiology* **156**: 1313-1322.

Breisch J, Huber LS, Kraiczy P, Hubloher J & Averhoff B (2022) The ß-ketoadipate pathway of *Acinetobacter baumannii* is involved in complement resistance and affects resistance against aromatic antibiotics. *Environmental Microbiology Reports* **14**: 170-178.

Bundy BM, Collier LS, Hoover TR & Neidle EL (2002) Synergistic transcriptional activation by one regulatory protein in response to two metabolites. *Proceedings of the National Academy of Sciences* **99**: 7693-7698.

Chen S, Cao L, Lv T, *et al.* (2024) Regulation mechanism of the long-chain n-alkane monooxygenase

gene *almA* in *Acinetobacter venetianus* RAG-1. *Applied and Environmental Microbiology* **91**: e02050-02024.

Cosper Nathaniel J, Collier Lauren S, Clark Todd J, Scott Robert A & Neidle Ellen L (2000) Mutations in *catB*, the Gene Encoding Muconate Cycloisomerase, Activate Transcription of the Distalben Genes and Contribute to a Complex Regulatory Circuit in *Acinetobacter* sp. Strain ADP1. *Journal of Bacteriology* **182**: 7044-7052.

Cunningham L, Gruer MJ & Guest JR (1997) Transcriptional regulation of the aconitase genes (*acnA* and *acnB*) of *Escherichia coli*. *Microbiology* **143**: 3795-3805.

D'Almeida AP, de Azevedo DCS, Melo VMM, de Albuquerque TL & Rocha MVP (2024) Bioemulsifier production by *Acinetobacter venetianus* AMO1502: Potential for bioremediation and environmentally friendly applications. *Marine Pollution Bulletin* **203**: 116436.

Dal S, Trautwein G & Gerischer U (2005) Transcriptional Organization of Genes for Protocatechuate and Quinate Degradation from *Acinetobacter* sp. Strain ADP1. *Applied and Environmental Microbiology* **71**: 1025-1034.

de Lorenzo V, Pérez-Pantoja D & Nikel Pablo I (2024) *Pseudomonas putida* KT2440: the long journey of a soil-dweller to become a synthetic biology chassis. *Journal of Bacteriology* **206**: e00136-00124.

Durot M, Le Fèvre F, de Berardinis V, Kreimeyer A, Vallenet D, Combe C, Smidtas S, Salanoubat M, Weissenbach J & Schachter V (2008) Iterative reconstruction of a global metabolic model of *Acinetobacter baylyi* ADP1 using high-throughput growth phenotype and gene essentiality data. *BMC Systems Biology* **2**: 85.

Fischer R, Bleichrodt FS & Gerischer UC (2008) Aromatic degradative pathways in *Acinetobacter baylyi* underlie carbon catabolite repression. *Microbiology* **154**: 3095-3103.

Hooppaw Anna J, McGuffey Jenna C, Di Venanzio G, Ortiz-Marquez Juan C, Weber Brent S, Lightly Tasia J, van Opijnen T, Scott Nichollas E, Cardona Silvia T & Feldman Mario F (2022) The Phenylacetic Acid Catabolic Pathway Regulates Antibiotic and Oxidative Stress Responses in *Acinetobacter*. *mBio* **13**: e01863-01821.

Hori K, Yamashita S, Ishii Si, Kitagawa M, Tanji Y & Unno H (2001) Isolation, Characterization and Application to Off-Gas Treatment of Toluene-Degrading Bacteria. *Journal of Chemical Engineering of Japan* **34**: 1120-1126.

Hori K, Ishikawa M, Yamada M, Higuchi A, Ishikawa Y & Ebi H (2011) Production of peritrichate bacterionanofibers and their proteinaceous components by *Acinetobacter* sp. Tol 5 cells affected by

growth substrates. *Journal of Bioscience and Bioengineering* **111**: 31-36.

Höring P, Rothschild-Mancinelli K, Sharma ND, Boyd DR & Allen CCR (2016) Oxidative biotransformations of phenol substrates catalysed by toluene dioxygenase: A molecular docking study. *Journal of Molecular Catalysis B: Enzymatic* **134**: 396-406.

Inoue S, Yoshimoto S & Hori K (2025) A new target of multiple lysine methylation in bacteria. *Journal of Bacteriology* **207**: e00325-00324.

Ishige T, Tani A, Sakai Y & Kato N (2000) Long-Chain Aldehyde Dehydrogenase That Participates in n-Alkane Utilization and Wax Ester Synthesis in *Acinetobacter* sp. Strain M-1. *Applied and Environmental Microbiology* **66**: 3481-3486.

Ishikawa M & Hori K (2021) Complete Genome Sequence of the Highly Adhesive Bacterium *Acinetobacter* sp. Strain Tol 5. *Microbiology Resource Announcements* **10**: 10.1128/mra.00567-00521.

Ishikawa M & Hori K (2024) The elimination of two restriction enzyme genes allows for electroporation-based transformation and CRISPR-Cas9-based base editing in the non-competent Gram-negative bacterium *Acinetobacter* sp. Tol 5. *Applied and Environmental Microbiology* **90**: e00400-00424.

Ishikawa M, Nakatani H & Hori K (2012) AtaA, a New Member of the Trimeric Autotransporter Adhesins from *Acinetobacter* sp. Tol 5 Mediating High Adhesiveness to Various Abiotic Surfaces. *PLOS ONE* **7**: e48830.

Ishikawa M, Shigemori K, Suzuki A & Hori K (2012) Evaluation of adhesiveness of *Acinetobacter* sp. Tol 5 to abiotic surfaces. *Journal of Bioscience and Bioengineering* **113**: 719-725.

Jiménez JI, Pérez-Pantoja D, Chavarría M, Díaz E & de Lorenzo V (2014) A second chromosomal copy of the *catA* gene endows *Pseudomonas putida* mt-2 with an enzymatic safety valve for excess of catechol. *Environmental Microbiology* **16**: 1767-1778.

Jordan P, Tang Y, Bradbury AJ, Thomson AJ & JR. G (1999) Biochemical and spectroscopic characterization of *Escherichia coli* aconitases (AcnA and AcnB). *The Biochemical journal* **344**: 739-746.

Kannisto MS, Mangayil RK, Shrivastava-Bhattacharya A, Pletschke BI, Karp MT & Santala VP (2015) Metabolic engineering of *Acinetobacter baylyi* ADP1 for removal of Clostridium butyricum growth inhibitors produced from lignocellulosic hydrolysates. *Biotechnology for Biofuels* **8**: 198.

Kong W, Zhao C, Gao X, Wang L, Tian Q, Liu Y, Xue S, Han Z, Chen F & Wang S (2021) Characterization and Transcriptome Analysis of a Long-Chain n-Alkane-Degrading Strain *Acinetobacter pittii* SW-1. *International Journal of Environmental Research and Public Health* **18**: 6365.

Kurnia K, Efimova E, Santala V & Santala S (2024) Metabolic engineering of *Acinetobacter baylyi* ADP1 for naringenin production. *Metabolic Engineering Communications* **19**: e00249.

Liew FE, Nogle R, Abdalla T, *et al.* (2022) Carbon-negative production of acetone and isopropanol by gas fermentation at industrial pilot scale. *Nature Biotechnology* **40**: 335-344.

Lin G-H, Hsieh M-C & Shu H-Y (2021) Role of Iron-Containing Alcohol Dehydrogenases in *Acinetobacter baumannii* ATCC 19606 Stress Resistance and Virulence. *International Journal of Molecular Sciences* **22**: 9921.

Liu H, Tao X, Ntakirutimana S, Liu Z-H, Li B-Z & Yuan Y-J (2024) Engineering *Pseudomonas putida* for lignin bioconversion into *cis-cis* muconic acid. *Chemical Engineering Journal* **495**: 153375.

Liu J, Zhao B, Lan Y & Ma T (2021) Enhanced degradation of different crude oils by defined engineered consortia of *Acinetobacter venetianus* RAG-1 mutants based on their alkane metabolism. *Bioresource Technology* **327**: 124787.

Liu J, Wang D, Tong R, Ye S, Zhao Y, Wu J & Gan Y (2025) Engineered Rhizobia with Trehalose-Producing Genes Enhance Peanut Growth Under Salinity Stress. *Agronomy* **15**: 974.

Luo J, McIntyre Emily A, Bedore Stacy R, Santala V, Neidle Ellen L & Santala S (2022) Characterization of Highly Ferulate-Tolerant *Acinetobacter baylyi* ADP1 Isolates by a Rapid Reverse Engineering Method. *Applied and Environmental Microbiology* **88**: e01780-01721.

Maier T, Förster H-H, Asperger O & Hahn U (2001) Molecular Characterization of the 56-kDa CYP153 from *Acinetobacter* sp. EB104. *Biochemical and Biophysical Research Communications* **286**: 652-658.

Martín-González J, Montero-Bullón J-F, Muñoz-Fernández G, Buey RM & Jiménez A (2025) Valorization of waste cooking oil for bioproduction of industrially-relevant metabolites in *Ashbya gossypii*. *New Biotechnology* **88**: 32-38.

Martínez-García E & de Lorenzo V (2024) *Pseudomonas putida* as a synthetic biology chassis and a metabolic engineering platform. *Current Opinion in Biotechnology* **85**: 103025.

Mateo-Estrada V, Graña-Miraglia L, López-Leal G & Castillo-Ramírez S (2019) Phylogenomics Reveals Clear Cases of Misclassification and Genus-Wide Phylogenetic Markers for *Acinetobacter*. *Genome Biology and Evolution* **11**: 2531-2541.

McClure R, Balasubramanian D, Sun Y, Bobrovskyy M, Sumby P, Genco CA, Vanderpool CK & Tjaden B (2013) Computational analysis of bacterial RNA-Seq data. *Nucleic Acids Research* **41**: e140-e140.

Morris FC, Jiang Y, Fu Y, Kostoulias X, Murray GL, Yu Y & Peleg AY (2024) Lactate metabolism

promotes in vivo fitness during *Acinetobacter baumannii* infection. *FEMS Microbiology Letters* **371**: fnae032.

Nakazawa T (2002) Travels of a *Pseudomonas*, from Japan around the world. *Environmental Microbiology* **4**: 782-786.

Nelson KE, Weinel C, Paulsen IT, *et al.* (2002) Complete genome sequence and comparative analysis of the metabolically versatile *Pseudomonas putida* KT2440. *Environmental Microbiology* **4**: 799-808.

Nie Y, Chi C-Q, Fang H, Liang J-L, Lu S-L, Lai G-L, Tang Y-Q & Wu X-L (2014) Diverse alkane hydroxylase genes in microorganisms and environments. *Scientific Reports* **4**: 4968.

Nogales J, García JL & Díaz E (2017) Degradation of Aromatic Compounds in *Pseudomonas*: A Systems Biology View. *Aerobic Utilization of Hydrocarbons, Oils and Lipids*,(Rojo F, ed.) pp. 1-49. Springer, Cham.

Ohara Y, Yoshimoto S & Hori K (2019) Control of AtaA-mediated bacterial immobilization by casein hydrolysates. *Journal of Bioscience and Bioengineering* **128**: 544-550.

Park C, Shin B & Park W (2019) Alternative fate of glyoxylate during acetate and hexadecane metabolism in *Acinetobacter oleivorans* DR1. *Scientific Reports* **9**: 14402.

Park C, Shin B, Jung J, Lee Y & Park W (2017) Metabolic and stress responses of *Acinetobacter oleivorans* DR1 during long-chain alkane degradation. *Microbial Biotechnology* **10**: 1809-1823.

Phale PS, Malhotra H & Shah BA (2020) Chapter One - Degradation strategies and associated regulatory mechanisms/features for aromatic compound metabolism in bacteria. *Advances in Applied Microbiology,* Vol. 112 (Gadd GM & Sariaslani S, eds.), pp. 1-65. Academic Press.

Pontrelli S, Chiu T-Y, Lan EI, Chen FYH, Chang P & Liao JC (2018) *Escherichia coli* as a host for metabolic engineering. *Metabolic Engineering* **50**: 16-46.

Ramos J-L, Sol Cuenca M, Molina-Santiago C, Segura A, Duque E, Gómez-García MR, Udaondo Z & Roca A (2015) Mechanisms of solvent resistance mediated by interplay of cellular factors in *Pseudomonas putida*. *FEMS Microbiology Reviews* **39**: 555-566.

Ren X & Palmer Lauren D (2023) *Acinetobacter* Metabolism in Infection and Antimicrobial Resistance. *Infection and Immunity* **91**: e00433-00422.

Rodríguez-Castro L, Durán RE, Méndez V, Dorochesi F, Zühlke D, Riedel K & Seeger M (2024) The long-chain flavodoxin FldX1 improves the biodegradation of 4-hydroxyphenylacetate and 3-hydroxyphenylacetate and counteracts the oxidative stress associated to aromatic catabolism in

Paraburkholderia xenovorans. *Biological Research* **57**: 12.

Rojo F (2009) Degradation of alkanes by bacteria. *Environmental Microbiology* **11**: 2477-2490.

Sabapathy PC, Devaraj S, Parthipan A & Kathirvel P (2019) Polyhydroxyalkanoate production from statistically optimized media using rice mill effluent as sustainable substrate with an analysis on the biopolymer's degradation potential. *International Journal of Biological Macromolecules* **126**: 977-986.

Sauer U & Eikmanns BJ (2005) The PEP—pyruvate—oxaloacetate node as the switch point for carbon flux distribution in bacteria: We dedicate this paper to Rudolf K. Thauer, Director of the Max-Planck-Institute for Terrestrial Microbiology in Marburg, Germany, on the occasion of his 65th birthday. *FEMS Microbiology Reviews* **29**: 765-794.

Sazykin I, Sazykina M, Khmelevtsova L, Khammami M, Karchava S, Zhuravleva M & Kudeevskaya E (2016) Expression of SOD and production of reactive oxygen species in *Acinetobacter calcoaceticus* caused by hydrocarbon oxidation. *Annals of Microbiology* **66**: 1039-1045.

Silva-Rocha R & de Lorenzo V (2012) A GFP-*lacZ* Bicistronic Reporter System for Promoter Analysis in Environmental Gram-Negative Bacteria. *PLOS ONE* **7**: e34675.

Spain JC, Zylstra GJ, Blake CK & Gibson DT (1989) Monohydroxylation of phenol and 2,5-dichlorophenol by toluene dioxygenase in *Pseudomonas putida* F1. *Applied and Environmental Microbiology* **55**: 2648-2652.

Stuani L, Lechaplais C, Salminen AV, *et al.* (2014) Novel metabolic features in *Acinetobacter baylyi* ADP1 revealed by a multiomics approach. *Metabolomics* **10**: 1223-1238.

Taboada B, Estrada K, Ciria R & Merino E (2018) Operon-mapper: a web server for precise operon identification in bacterial and archaeal genomes. *Bioinformatics* **34**: 4118-4120.

Taeger K, Knackmuss H-J & Schmidt E (1988) Biodegradability of mixtures of chloro- and methylsubstituted aromatics: Simultaneous degradation of 3-chlorobenzoate and 3-methylbenzoate. *Applied Microbiology and Biotechnology* **28**: 603-608.

Teufel R, Mascaraque V, Ismail W, Voss M, Perera J, Eisenreich W, Haehnel W & Fuchs G (2010) Bacterial phenylalanine and phenylacetate catabolic pathway revealed. *Proceedings of the National Academy of Sciences* **107**: 14390-14395.

Usami A, Ishikawa M & Hori K (2020) Gas-phase bioproduction of a high-value-added monoterpenoid (*E*)-geranic acid by metabolically engineered *Acinetobacter* sp. Tol 5. *Green Chemistry* **22**: 1258-1268.

van Beilen Jan B, Funhoff Enrico G, van Loon A, Just A, Kaysser L, Bouza M, Holtackers R,

Röthlisberger M, Li Z & Witholt B (2006) Cytochrome P450 Alkane Hydroxylases of the CYP153 Family Are Common in Alkane-Degrading Eubacteria Lacking Integral Membrane Alkane Hydroxylases. *Applied and Environmental Microbiology* **72**: 59-65.

Vijayakumar S, Indranil B & Veeraraghavan B (2019) Accurate Identification of Clinically Important *Acinetobacter* Spp.: An Update. *Future Science OA* **5**: FSO395.

Wang Y, Wang Z, Chen Y, Hua X, Yu Y & Ji Q (2019) A Highly Efficient CRISPR-Cas9-Based Genome Engineering Platform in *Acinetobacter baumannii* to Understand the H_2O_2-Sensing Mechanism of OxyR. *Cell Chemical Biology* **26**: 1732-1742.e1735.

Wohlfarth S, Hoesche C, Strunk C & Winkler UK (1992) Molecular genetics of the extracellular lipase of *Pseudomonas aeruginosa* PAO1. *Microbiology* **138**: 1325-1335.

Yoshimoto S, Ohara Y, Nakatani H & Hori K (2017) Reversible bacterial immobilization based on the salt-dependent adhesion of the bacterionanofiber protein AtaA. *Microbial Cell Factories* **16**: 123.

Yoshimoto S, Hattori M, Inoue S, Mori S, Ohara Y & Hori K (2025) Identification of toluene degradation genes in *Acinetobacter* sp. Tol 5. *Journal of Bioscience and Bioengineering* **140**: 284-289.

Yoshimoto S, Aoki S, Ohara Y, Ishikawa M, Suzuki A, Linke D, Lupas AN & Hori K (2023) Identification of the adhesive domain of AtaA from *Acinetobacter* sp. Tol 5 and its application in immobilizing *Escherichia coli*. *Frontiers in Bioengineering and Biotechnology* **10**:1095057.

Yoshimoto S, Ishii S, Kawashiri A, Matsushita T, Linke D, Göttig S, Kempf VAJ, Takai M & Hori K (2024) Adhesion preference of the sticky bacterium *Acinetobacter* sp. Tol 5. *Frontiers in Bioengineering and Biotechnology* **12**: 1342418.

Yu H, Peng Z, Zhan Y, *et al.* (2011) Novel Regulator MphX Represses Activation of Phenol Hydroxylase Genes Caused by a XylR/DmpR-Type Regulator MphR in *Acinetobacter calcoaceticus*. *PLOS ONE* **6**: e17350.

Zeidler S, Hubloher J, Schabacker K, Lamosa P, Santos H & Müller V (2017) Trehalose, a temperature- and salt-induced solute with implications in pathobiology of *Acinetobacter baumannii*. *Environmental Microbiology* **19**: 5088-5099.

Zhao Y, Wei H-M, Yuan J-L, Xu L & Sun J-Q (2023) A comprehensive genomic analysis provides insights on the high environmental adaptability of *Acinetobacter* strains. *Frontiers in Microbiology* **14**: 1177951.

Zylstra GJ, McCombie WR, Gibson DT & Finette BA (1988) Toluene degradation by *Pseudomonas putida* F1: genetic organization of the tod operon. *Applied and Environmental Microbiology* **54**:

1498-1503.

FIGURE LEGENDS

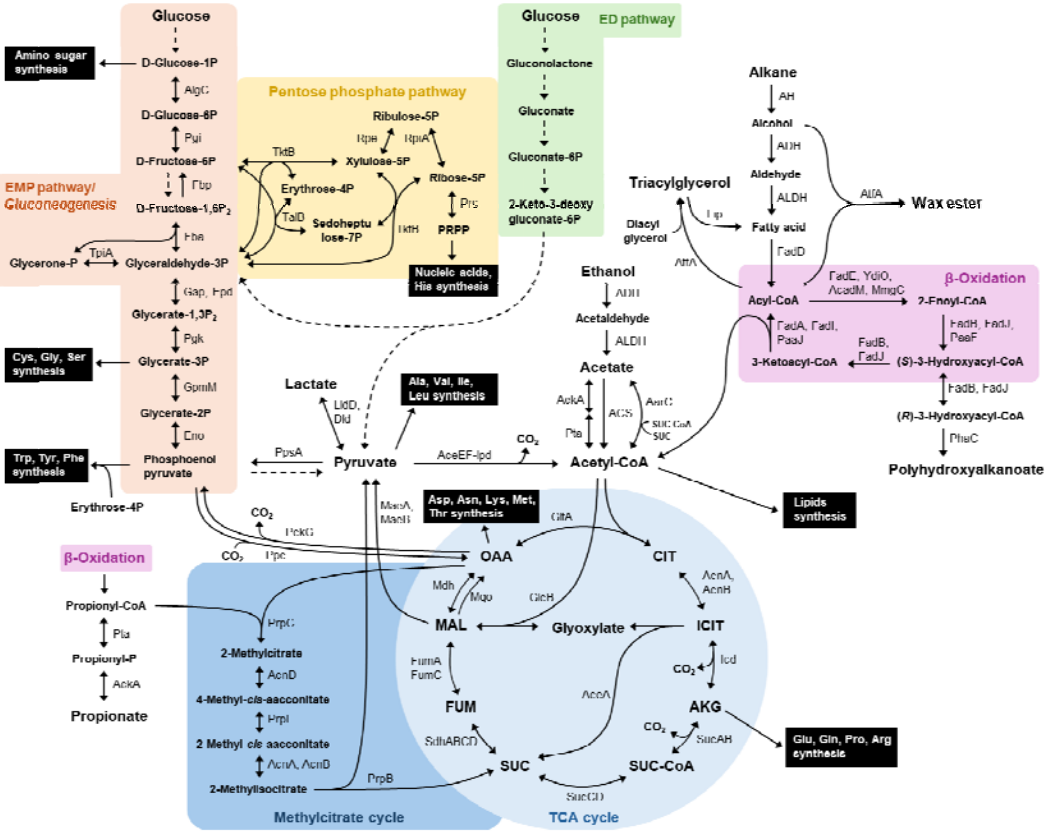

Fig. 1. Prediction of the central metabolic pathway of *Acinetobacter* sp. Tol 5. Genes related to the central metabolic pathway were analyzed and listed in Table S4. Dashed arrows indicate metabolic reactions for which the corresponding genes are not found in Tol 5 genome. Abbreviations: ADH; alcohol dehydrogenase, AH; alkane hydroxylase, AKG; α-ketoglutarate, ALDH; aldehyde dehydrogenase, CIT; citrate, FUM; fumarate, ICIT; isocitrate, MAL; malate, OAA; oxaloacetate, PRPP; phosphoribosyl pyrophosphate, SUC; succinate, SUC-CoA; succinyl-CoA.

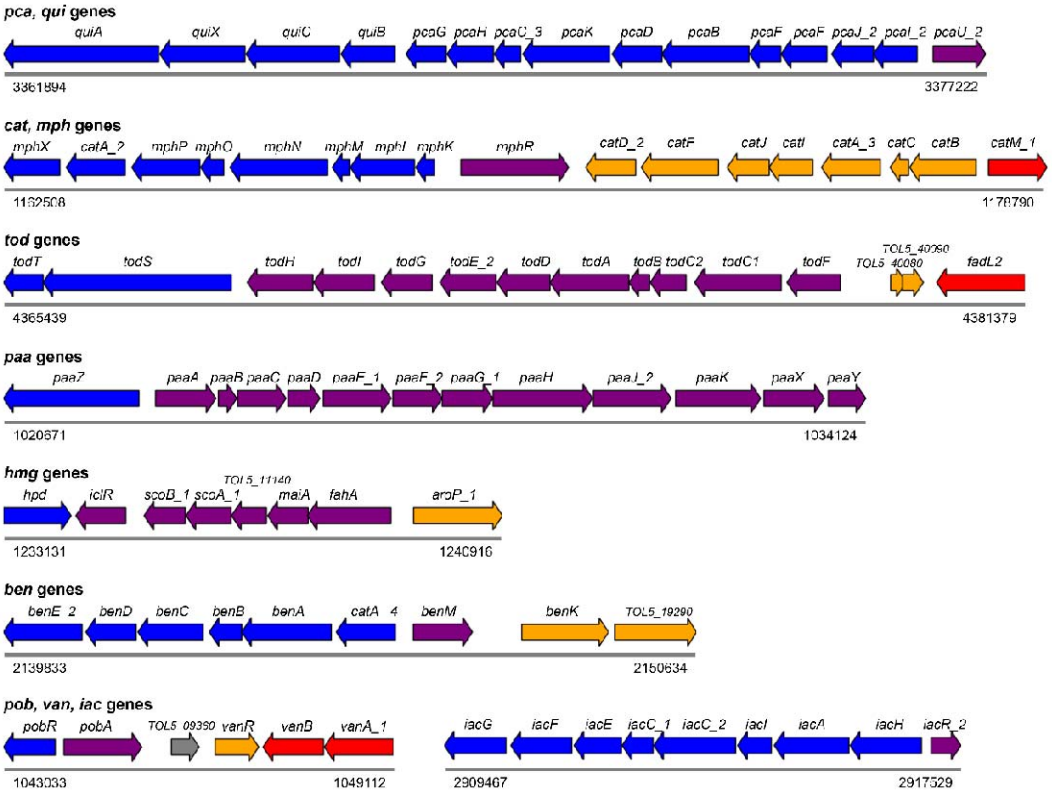

Fig. 2. Genetic organization of genes involved in the degradation of aromatic compounds in *Acinetobacter* sp. Tol 5. Predicted operon structures are illustrated based on analyses using Operon-mapper and Rockhopper. Genes within the same operon are represented by arrows of the same color. Proposed gene names or predicted functions are labeled above each arrow, and genomic coordinates are indicated below.

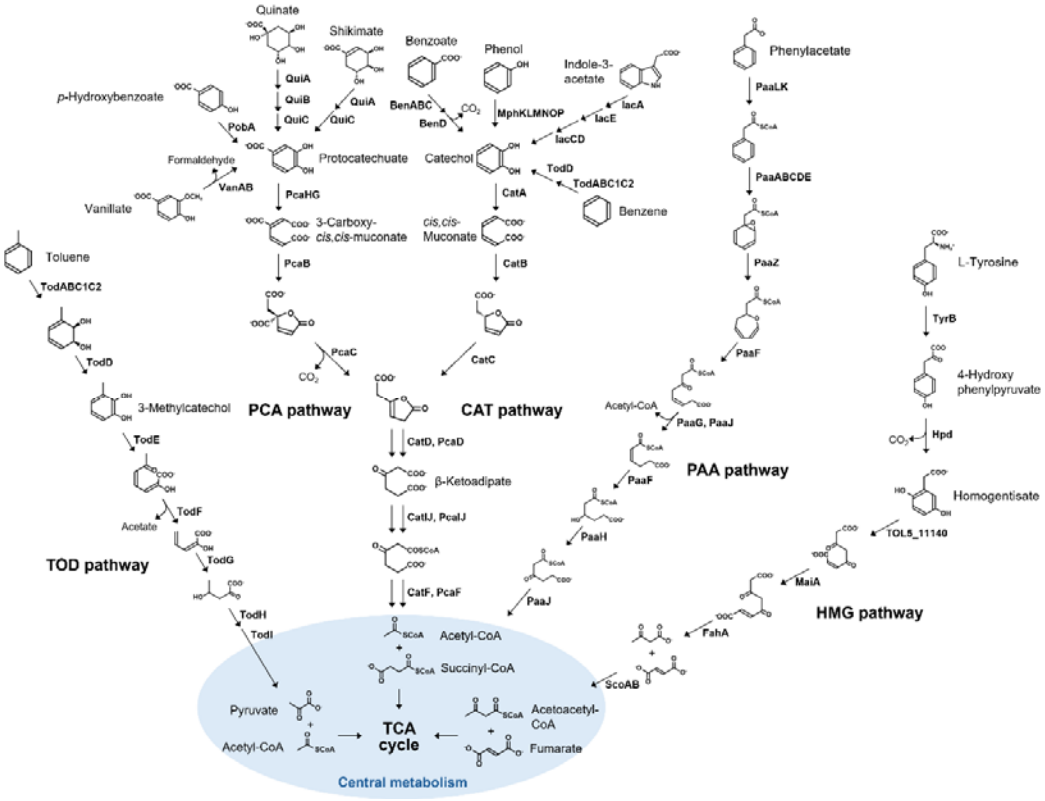

Fig. 3. Predicted degradation pathways of aromatic compounds in *Acinetobacter* sp. Tol 5, reconstructed based on the genes shown in Fig. 2 and Table S4. Question marks and dashed arrows indicate steps for which the genes encoding the corresponding enzymes have not been identified in Tol 5.

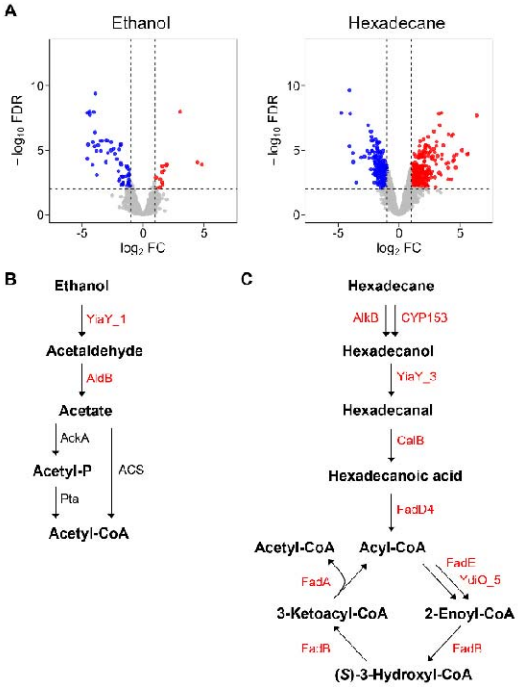

Fig. 4. Transcriptome analysis of *Acinetobacter* sp. Tol 5 grown on lactate, ethanol, and hexadecane. (**A**) Volcano plots comparing gene expression between lactate and ethanol (left) or hexadecane (right) as sole carbon sources (n = 3 biologically independent samples). Red and blue dots represent significantly upregulated and downregulated genes, respectively (FDR < 0.01, |log□ FC| > 1). (**B**, **C**) Proposed ethanol (**B**) and hexadecane (**C**) degradation pathways in Tol 5 based on transcriptome analysis. Genes encoding enzymes significantly upregulated under each condition are shown in red.

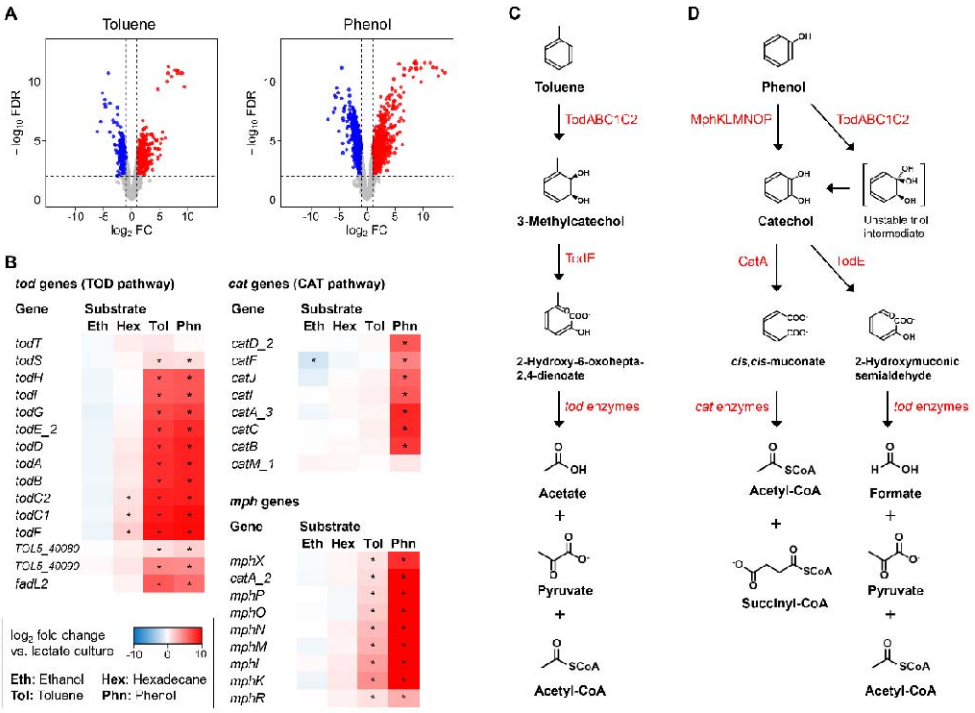

Fig. 5. Differential gene expression of *Acinetobacter sp*. Tol 5 grown on various aromatics, ethanol, and hexadecane, using lactate as the reference condition. (**A**) Volcano plots comparing gene expression between lactate and toluene (left) or phenol (right) as sole carbon sources (n = 3 biologically independent samples). Red and blue dots represent significantly upregulated and downregulated genes, respectively (FDR < 0.01, |log□ FC| > 1). (**B**) Heat maps showing the average log□ FC of the genes involved in the degradation of toluene and phenol (*tod*, *cat*, and *mph* genes). The color gradient indicates the magnitude of the log□ FC values, with the deepest red representing ≥ 10 and the deepest blue representing ≤ -10. Asterisks (*) denote differentially expressed genes defined by $|\log_2 FC| > 1$, $\log_2 CPM > 3$, and FDR < 0.01. (**C, D**) Proposed degradation pathways of toluene (**C**) and phenol (**D**) in Tol 5 based on transcriptome data. Genes encoding enzymes significantly upregulated under each condition are shown in red.

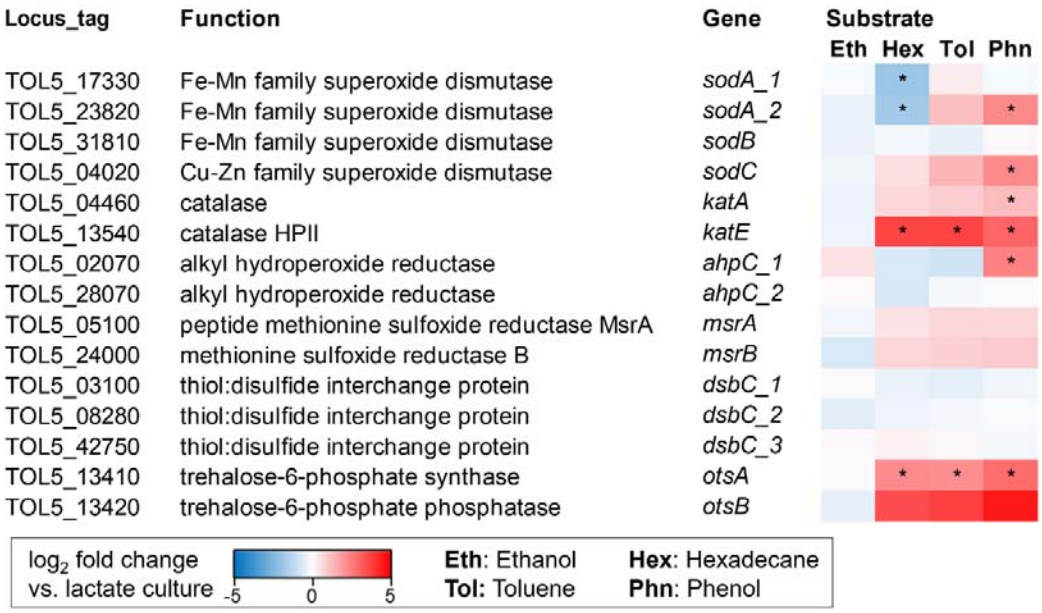

Fig. 6. Heat map showing the average $\log_2$ FC of genes involved in oxidative stress and osmotic stress resistance. The color gradient indicates the magnitude of the log□ FC values, with the deepest red representing ≥ 5 and the deepest blue representing ≤ –5. Asterisks (*) denote differentially expressed genes defined by $|\log_2 \text{FC}| > 1$, $\log_2 \text{CPM} > 3$, and FDR < 0.01.

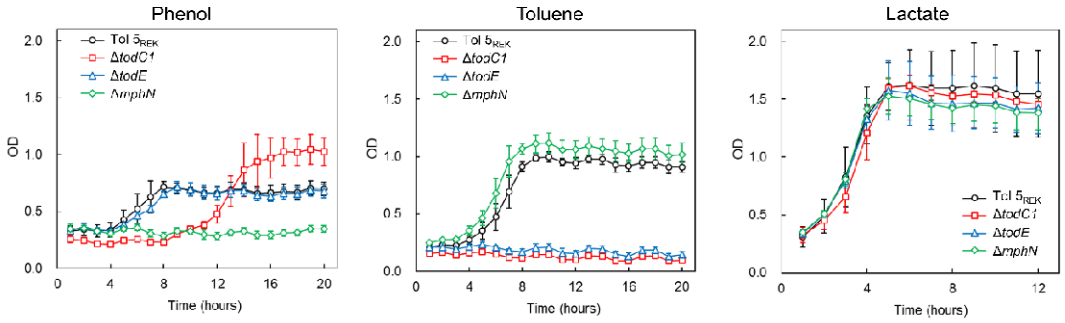

Fig. 7. Growth on different carbon sources. Tol 5_{REK} (circles), the Δ*todC1* mutant (squares), the Δ*todE* mutant (triangles), and the Δ*mphN* mutant (diamonds) were inoculated to BS medium containing phenol, toluene, or sodium lactate at a carbon equivalent concentration of 1.4×10^{-2} mol/L. Data are presented as the means ± SEMs (biological replicates n = 3).

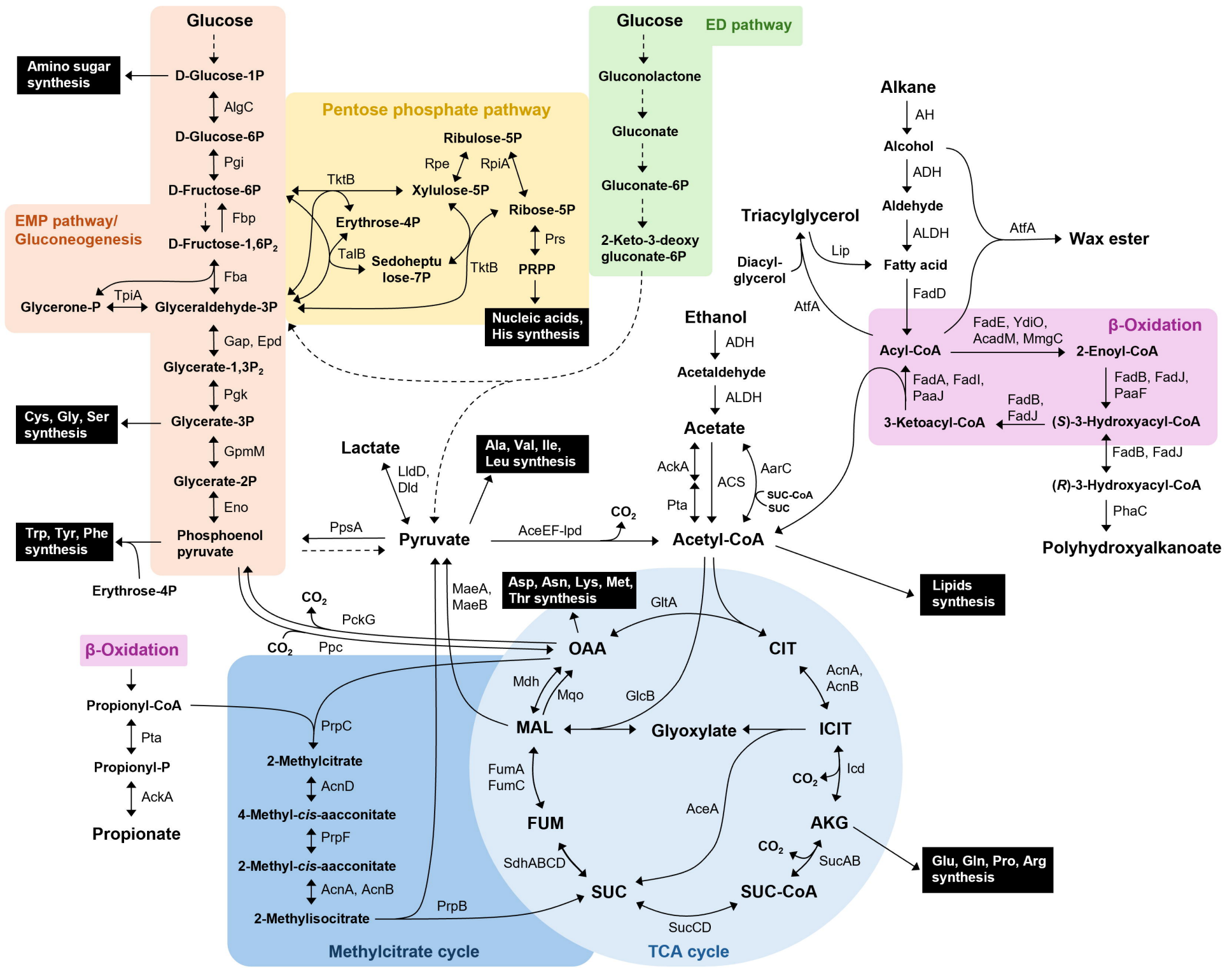
Glucose
Amino sugar synthesis
D-Glucose-1P
AlgC
D-Glucose-6P
Pgi
D-Fructose-6P
Fbp
EMP pathway/ Gluconeogenesis
D-Fructose-1,6P2
Fba
Glycerone-P
TpiA
Glyceraldehyde-3P
Gap, Epd
Glycerate-1,3P2
Pgk
Cys, Gly, Ser synthesis
Glycerate-3P
GpmM
Glycerate-2P
Eno
Trp, Tyr, Phe synthesis
Phosphoenol pyruvate
Erythrose-4P
Pentose phosphate pathway
Ribulose-5P
Rpe
RpiA
TktB
Xylulose-5P
Ribose-5P
Erythrose-4P
TalB
Sedoheptulose-7P
TktB
Prs
PRPP
Nucleic acids, His synthesis
Glucose
ED pathway
Gluconolactone
Gluconate
Gluconate-6P
2-Keto-3-deoxy gluconate-6P
Alkane
AH
Alcohol
ADH
Aldehyde
ALDH
Fatty acid
FadD
AtfA
Wax ester
Triacylglycerol
Lip
Diacyl-glycerol
AtfA
Acyl-CoA
FadE, YdiO, AcadM, MmgC
β-Oxidation
2-Enoyl-CoA
FadB, FadJ, PaaF
FadA, FadI, PaaJ
FadB, FadJ
3-Ketoacyl-CoA
(S)-3-Hydroxyacyl-CoA
FadB, FadJ
(R)-3-Hydroxyacyl-CoA
PhaC
Polyhydroxyalkanoate
Ethanol
ADH
Acetaldehyde
ALDH
Acetate
AckA
ACS
AarC
Pta
SUC-CoA
SUC
Lactate
LldD, Dld
Ala, Val, Ile, Leu synthesis
PpsA
Pyruvate
AceEF-lpd
CO2
Acetyl-CoA
Lipids synthesis
MaeA, MaeB
Asp, Asn, Lys, Met, Thr synthesis
GltA
CO2
PckG
CO2
Ppc
OAA
CIT
AcnA, AcnB
Mdh
Mqo
GlcB
MAL
Glyoxylate
ICIT
β-Oxidation
Propionyl-CoA
Pta
Propionyl-P
AckA
Propionate
PrpC
2-Methylcitrate
AcnD
4-Methyl-cis-aacconitate
PrpF
2-Methyl-cis-aacconitate
AcnA, AcnB
2-Methylisocitrate
PrpB
FumA
FumC
FUM
CO2
Icd
AceA
AKG
CO2
SucAB
SdhABCD
SUC
SUC-CoA
SucCD
Glu, Gln, Pro, Arg synthesis
Methylcitrate cycle
TCA cycle

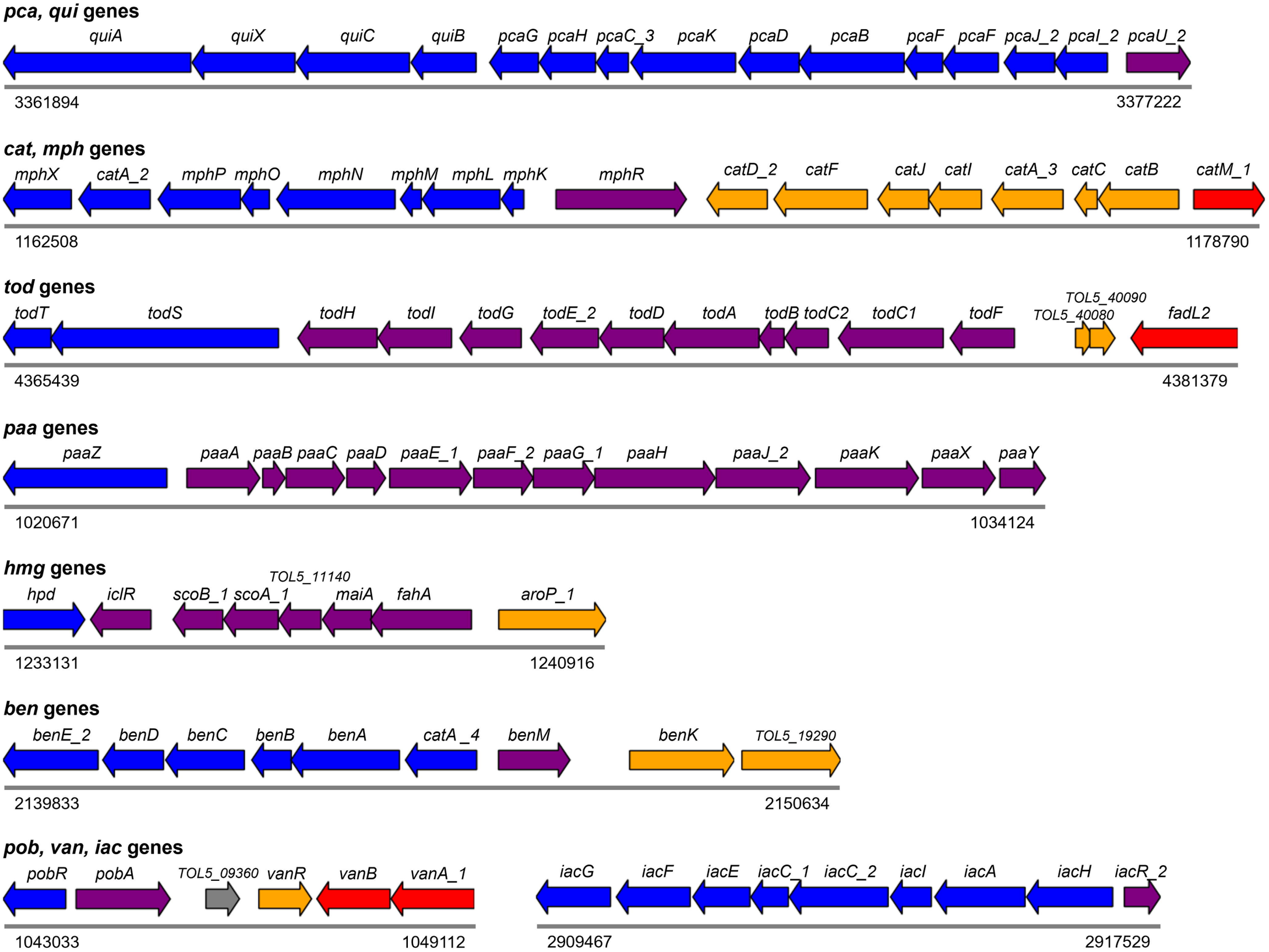
pca, qui genes
quiA
quiX
quiC
quiB
pcaG
pcaH
pcaC_3
pcaK
pcaD
pcaB
pcaF
pcaF
pcaJ_2
pcaI_2
pcaU_2
3361894
3377222
cat, mph genes
mphX
catA_2
mphP
mphO
mphN
mphM
mphL
mphK
mphR
catD_2
catF
catJ
catI
catA_3
catC
catB
catM_1
1162508
1178790
tod genes
todT
todS
todH
todI
todG
todE_2
todD
todA
todB
todC2
todC1
todF
TOL5_40090
TOL5_40080
fadL2
4365439
4381379
paa genes
paaZ
paaA
paaB
paaC
paaD
paaE_1
paaF_2
paaG_1
paaH
paaJ_2
paaK
paaX
paaY
1020671
1034124
hmg genes
hpd
iclR
scoB_1
TOL5_11140
scoA_1
maiA
fahA
aroP_1
1233131
1240916
ben genes
benE_2
benD
benC
benB
benA
catA _4
benM
benK
TOL5_19290
2139833
2150634
pob, van, iac genes
pobR
pobA
TOL5_09360
vanR
vanB
vanA_1
1043033
1049112
iacG
iacF
iacE
iacC_1
iacC_2
iacI
iacA
iacH
iacR_2
2909467
2917529

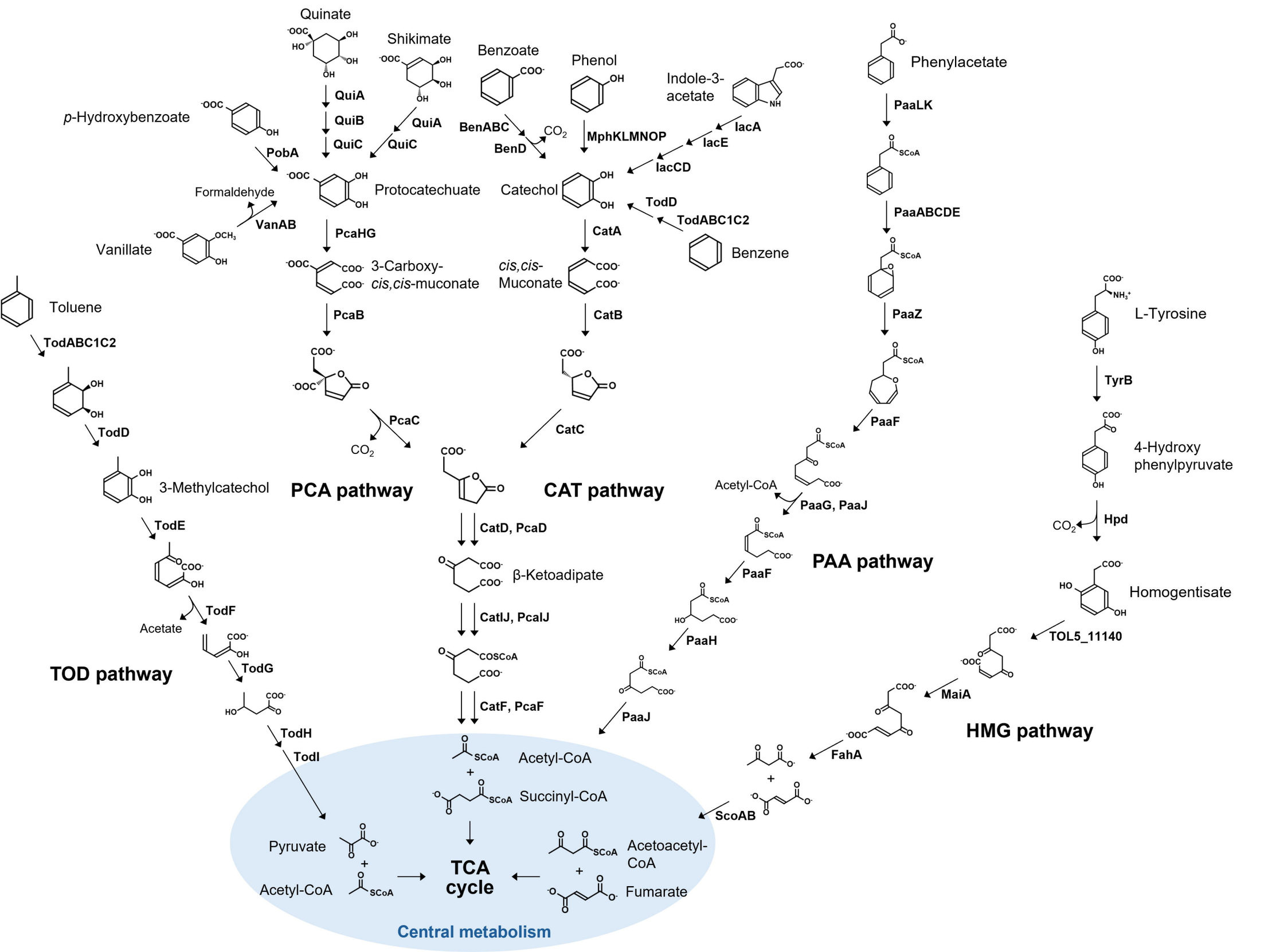
Quinate
Shikimate
Benzoate
Phenol
Indole-3-acetate
Phenylacetate
p-Hydroxybenzoate
QuiA
QuiB
QuiC
PobA
BenABC
BenD
CO2
MphKLMNOP
IacA
IacE
IacCD
Protocatechuate
Catechol
Formaldehyde
VanAB
Vanillate
TodD
TodABC1C2
Benzene
PcaHG
CatA
3-Carboxy-cis,cis-muconate
cis,cis-Muconate
PaaLK
PaaABCDE
PaaZ
PaaF
PcaB
CatB
Toluene
TodABC1C2
TodD
PcaC
CO2
CatC
3-Methylcatechol
PCA pathway
CAT pathway
Acetyl-CoA
PaaG, PaaJ
PAA pathway
L-Tyrosine
TyrB
4-Hydroxy phenylpyruvate
Hpd
CO2
Homogentisate
TOL5_11140
TodE
CatD, PcaD
β-Ketoadipate
PaaF
TodF
Acetate
CatIJ, PcaIJ
PaaH
TOD pathway
TodG
CatF, PcaF
PaaJ
MaiA
HMG pathway
TodH
TodI
Acetyl-CoA
Succinyl-CoA
FahA
ScoAB
Pyruvate
Acetyl-CoA
TCA cycle
Acetoacetyl-CoA
Fumarate
Central metabolism

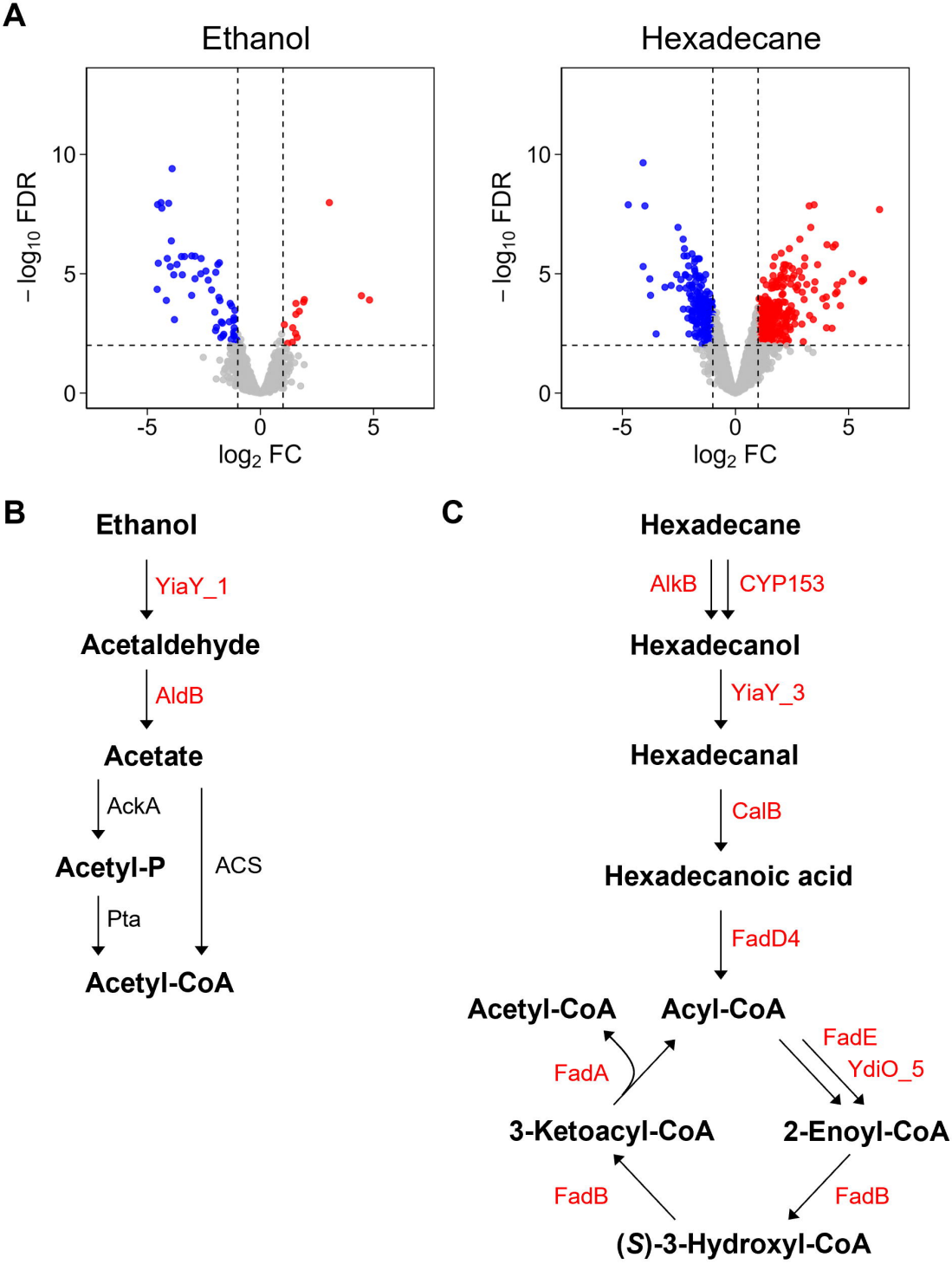
A
Ethanol
Hexadecane
$-\log_{10}$ FDR
$\log_2$ FC
10
5
0
-5
0
5
B
Ethanol
YiaY_1
Acetaldehyde
AldB
Acetate
AckA
ACS
Acetyl-P
Pta
Acetyl-CoA
C
Hexadecane
AlkB
CYP153
Hexadecanol
YiaY_3
Hexadecanal
CalB
Hexadecanoic acid
FadD4
Acetyl-CoA
Acyl-CoA
FadA
FadE
YdiO_5
3-Ketoacyl-CoA
2-Enoyl-CoA
FadB
FadB
(S)-3-Hydroxyl-CoA

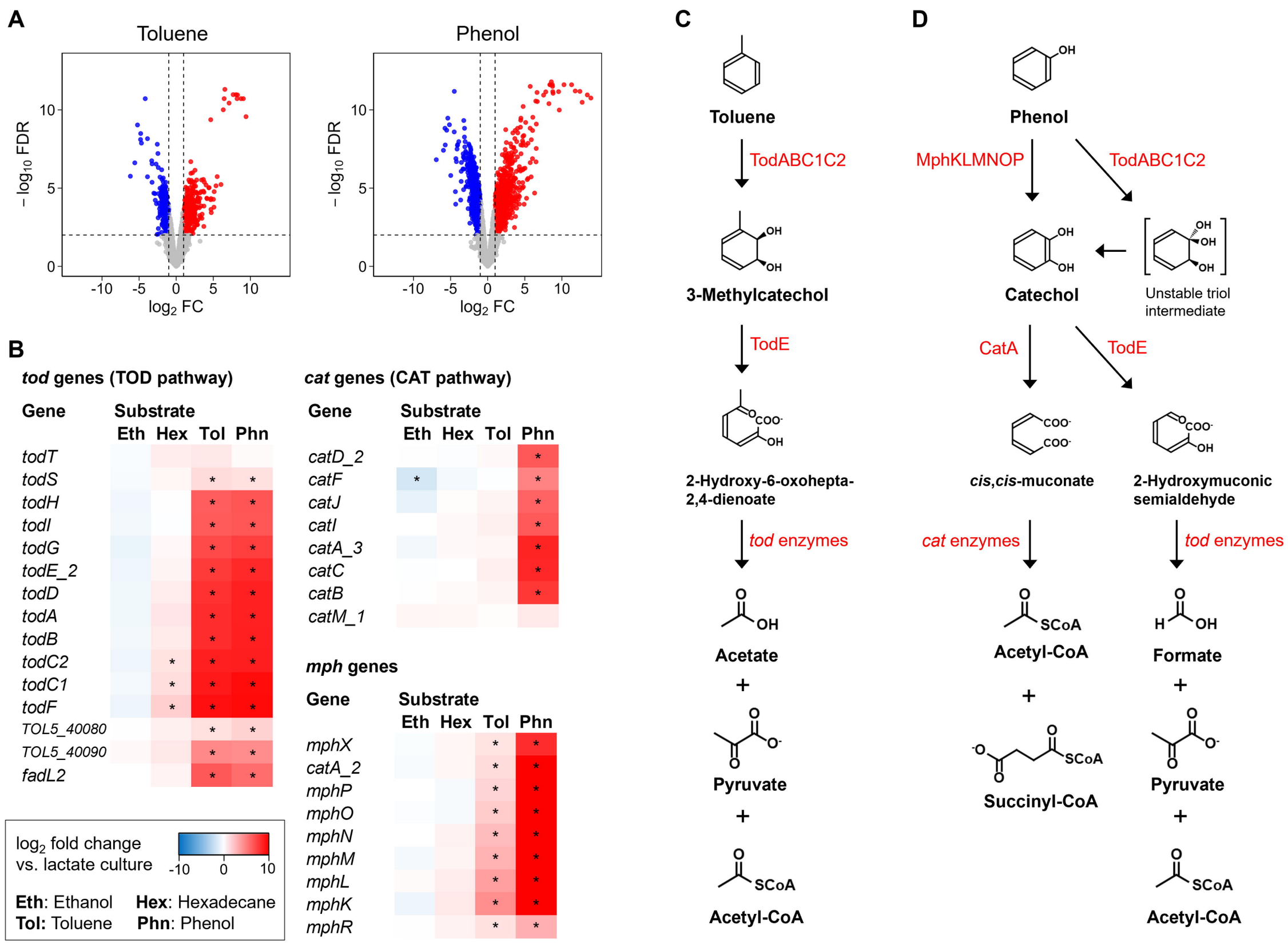
A
Toluene
Phenol
– log10 FDR
log2 FC
B
tod genes (TOD pathway)
Gene
Substrate
Eth Hex Tol Phn
todT
todS
todH
todI
todG
todE_2
todD
todA
todB
todC2
todC1
todF
TOL5_40080
TOL5_40090
fadL2
cat genes (CAT pathway)
catD_2
catF
catJ
catI
catA_3
catC
catB
catM_1
mph genes
mphX
catA_2
mphP
mphO
mphN
mphM
mphL
mphK
mphR
log2 fold change vs. lactate culture
Eth: Ethanol
Hex: Hexadecane
Tol: Toluene
Phn: Phenol
C
Toluene
TodABC1C2
3-Methylcatechol
TodE
2-Hydroxy-6-oxohepta-2,4-dienoate
tod enzymes
Acetate
Pyruvate
Acetyl-CoA
D
Phenol
MphKLMNOP
TodABC1C2
Catechol
Unstable triol intermediate
CatA
TodE
cis,cis-muconate
2-Hydroxymuconic semialdehyde
cat enzymes
tod enzymes
Acetyl-CoA
Succinyl-CoA
Formate
Pyruvate
Acetyl-CoA

Locus_tag	Function	Gene	Substrate			
			Eth	Hex	Tol	Phn
TOL5_17330	Fe-Mn family superoxide dismutase	*sodA_1*		*		
TOL5_23820	Fe-Mn family superoxide dismutase	*sodA_2*		*		*
TOL5_31810	Fe-Mn family superoxide dismutase	*sodB*				
TOL5_04020	Cu-Zn family superoxide dismutase	*sodC*				*
TOL5_04460	catalase	*katA*				*
TOL5_13540	catalase HPII	*katE*		*	*	*
TOL5_02070	alkyl hydroperoxide reductase	*ahpC_1*				*
TOL5_28070	alkyl hydroperoxide reductase	*ahpC_2*				
TOL5_05100	peptide methionine sulfoxide reductase MsrA	*msrA*				
TOL5_24000	methionine sulfoxide reductase B	*msrB*				
TOL5_03100	thiol:disulfide interchange protein	*dsbC_1*				
TOL5_08280	thiol:disulfide interchange protein	*dsbC_2*				
TOL5_42750	thiol:disulfide interchange protein	*dsbC_3*				
TOL5_13410	trehalose-6-phosphate synthase	*otsA*		*	*	*
TOL5_13420	trehalose-6-phosphate phosphatase	*otsB*				

$\log_2$ fold change vs. lactate culture

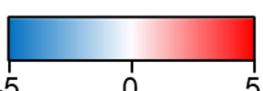

Eth: Ethanol **Hex**: Hexadecane
Tol: Toluene **Phn**: Phenol

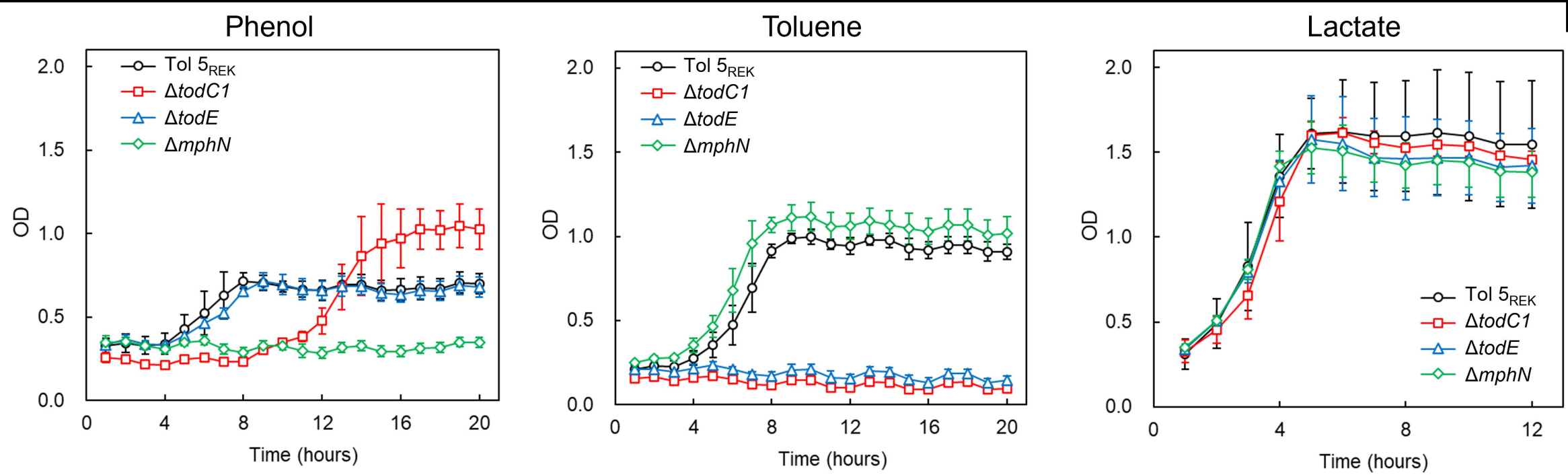
Phenol
Toluene
Lactate
Tol 5REK
ΔtodC1
ΔtodE
ΔmphN
OD
Time (hours)
0.0
0.5
1.0
1.5
2.0
0
4
8
12
16
20